A low-field approach to the transverse-field long-range Ising model on infinite-cylinder triangular lattices

Bachelorarbeit aus der Physik

vorgelegt von

Jan Alexander Koziol

18. Juni 2018

Institut für Theoretische Physik I
Friedrich-Alexander-Universität Erlangen-Nürnberg

Betreuer:
Prof. Dr. Kai Phillip Schmidt
M. Sc. Sebastian Fey

Abstract

This bachelor thesis has the aim to investigate further aspects of the ground-state properties of the frustrated antiferromagnetic transverse-field long-range Ising model on a triangular lattice with periodic boundary conditions in one direction. At first, we extend the existing studies on that cylindric lattice configuration made by Saadatmand, Bartlett and McCulloch by the ground-state analysis of the zero-field long-range Ising coupling directly in the diagonal basis. This analysis leads to a distinction between different columnar orders for different cylinder circumferences and a new first-order phase transition for an increasing long-range coupling decay exponent α. The behaviour of these stripe phases is also investigated with respect to quantum fluctuations induced by a small transverse field. This leads to the stability of the columnar zero-field ground state against a transverse field, in the case of long-range couplings. At second, an effective spin model for the ground state of the long-range transverse-field Ising model is derived with the use of Takahashi's perturbation theory about the limit of isolated rings. This model can describe the coupling between rings of the cylindric triangular lattice and shows a different behaviour than the first-order phase transition between the columnar orders if a transverse field is present. The model also shows that the chosen low-field ground-state space is not capable of forming a clock order.

Erklärung

Ich versichere, dass ich meine Bachelorarbeit ohne Hilfe Dritter und ohne Benutzung anderer als der angegebenen Quellen und Hilfsmittel angefertigt habe und die aus benutzten Quellen wörtlich oder inhaltlich entnommenen Stellen als solche kenntlich gemacht habe. Diese Arbeit hat in gleicher oder ähnlicher Form noch keiner Prüfungsbehörde vorgelegen.

Nürnberg, den 18. Juni 2018

Jan Koziol

Contents

1 Introduction and motivation

Quantum magnetism as a melange of quantum mechanics, statistical physics, and solid state physics has been an interesting and fascinating field of research for more than a hundred years, and it is still a bleeding edge research field. The ongoing interest in this field results in a large variety of different models which could be applied to an even larger variety of lattice types to generate different phenomena. Three key aspects which made the field of theoretical analysis of spin systems even more attractive in the last two decades are, at first the massive increase of available computation power which makes it possible to simulate even larger and more complex systems that are closer to the thermodynamical limit. The second important point is the experimental progress which makes it possible to construct spin-lattices in Penning traps as described by Britton [1]. Therefore the theoretical models can be compared to the experiment. The third point is quantum computation and quantum data storage, which require the investigation of all kinds of lattice types and spin-coupling models to find phases that could realise the complex computation or data-storing models in a simpler non-artificial way.
In this bachelor thesis, the main subject of study is the long-range transverse-field Ising Hamiltonian, applied on a triangular lattice with spin-$\frac{1}{2}$ lattice-sites and periodic boundary conditions in one lattice direction (see Fig. 3). This specific cylindric lattice structure is called YC(n)-lattice and will later be discussed in detail.
The main motivation of this thesis is the work of Saadatmand, Bartlett, and McCulloch in reference [2], who choose this cylindric structure to explore the properties of the long-range Ising model for the 2D triangular lattice and found an interesting new columnar phase (see fig. 5) which was not found in other studies on this 2D model (e. g. [3]). The other phases that were found on the YC(6)-lattice like a polarised phase at a high transverse field and a $\sqrt{3}\times\sqrt{3}$-clock order at rather short-range Ising interactions were confirmed by the studies of Fey, Kapfer and Schmidt in reference [3]. In this thesis, the primary approach is at first the analysis of the zero-field long-range Ising model ground state on different YC(n) structures to evaluate which spin configurations are energetically beneficial. This approach investigates large finite systems with periodic boundary conditions. The zero-field ground state shows a non-trivial behaviour of some columnar configurations on different YC(n) structures for different coupling decay exponents α, and even a first order phase transition.
The other aspect is an approach that exploits the loss of one dimension between the triangular lattice and the YC(n) structure due to the finite extension in one direction. This approach derives an effective 1D spin model for the ground states of super-sites (so-called rings) to understand the different processes and couplings between them. The derivation of this model is done perturbatively about the limit of isolated rings.
To understand the results presented in this thesis, in the next chapter there will be an introduction to the Ising Hamilton operator and a description of the triangular lattice and the YC(n)-lattice used in this thesis. After this recapitulation of the underlying physical setting in chapter 2, the current research results are presented for the triangular lattice and the YC(6)-lattice in chapter 3 to get a better picture of the whole system and its features. Then the new findings made within this thesis are presented and discussed in the context of the current research status for both the 2D triangular lattice and the YC(6) structure. The last point of this thesis is

a summary and an outlook (see chapter 7) to other perturbative approaches that could be done to gain more information about the $\sqrt{3} \times \sqrt{3}$-clock order.

2 Physical fundamentals

2.1 The transverse-field long-range Ising Hamiltonian

Ernst Ising introduced the nearest-neighbour Ising model in 1925 [4], but it was suggested earlier by Wilhelm Lenz in 1920 [5]. This model is one of the first ones to describe the magnetic behaviour of solid materials by taking the interaction between different spin-$\frac{1}{2}$ and the interaction between spins and an external field into account. The simplest form of that model is the parallel-field nearest-neighbour Ising model with the following Hamiltonian [6],

$$H = h \sum_i \sigma_i^z + J \sum_{<i,j>} \sigma_i^z \sigma_j^z \ . \tag{1}$$

The first sum takes the interaction between each spin and the external field into account. The second summation runs over all nearest neighbours and describes the coupling between the spins. In case of J being positive, equation 1 describes antiferromagnetic behaviour. To describe ferromagnetic behaviour, J has to be negative.
The next step is to develop the transverse-field Ising model. In this setting, the external magnetic field is applied orthogonally to the quantisation axis of the spin-spin coupling. Therefore the Hamilton operator is modified in the following way [7],

$$H = h \sum_i \sigma_i^x + J \sum_{<i,j>} \sigma_i^z \sigma_j^z \ . \tag{2}$$

The nearest-neighbour model is in most cases well understood (e. g. for the triangular lattice [8][9][10]) and is better approachable by numerical methods than the long-range coupling, because of the number of summations that have to be evaluated scales with the system size and the number of nearest neighbours.
Due to increasing computing power and experimental achievements in the simulation of spin systems with ion traps, as described by Britton et al. [1], the current studies on the Ising model also take mutual spin interactions of all spins on the lattice into account. The coupling decreases with the distance between the spins δ_{ij} according to a power law depending on the coupling decay exponent α. This modification leads to the following Hamiltonian [2],

$$H = h \sum_i \sigma_i^x + J \sum_{i>j} \frac{1}{|\delta_{i,j}|^\alpha} \sigma_i^z \sigma_j^z \tag{3}$$

In the following we focus on the ground state of the antiferromagnetic Hamiltonian at temperature zero.
It is also important to mention that the evaluation of equation 3 on different lattice models leads to a variety of different phases and phase transitions for different parameters. Therefore it is not enough to introduce only the Hamilton operator, but also necessary to describe the lattice on which the Hamiltonian is applied.

2.2 The YC(n) structure

Motivated by the work of Saadatmand, Barlett and McCulloch [2] the Hamiltonian described in equation 3 is applied on a triangular lattice with periodic boundary conditions in one direction after n spin-sites. This boundary condition leads to an n-leg cylinder build from the triangular lattice. To fully understand the properties of the system we will now discuss the features of the triangular lattice and how to derive the n-leg cylinder from it. There will also be a discussion of the unit cell used for further evaluations and the symmetries of the whole system.

2.2.1 The triangular lattice and geometrical frustration

The triangular lattice is one of the five Bravais lattices in 2D. Figure 1 shows an excerpt of the lattice. Its primary characteristic is that it consists out of equilateral triangles with an angle of $\frac{\pi}{3}$. The main difference between the triangular lattice and the square lattices is the fact that every lattice site has six nearest neighbours, and that on a triangular lattice closed loops with an odd length exist.

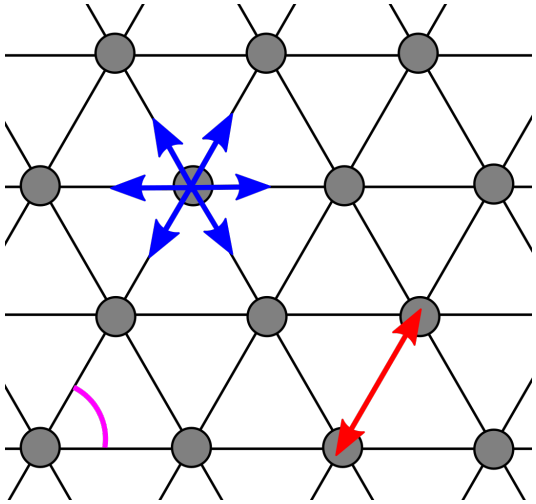

Figure 1: Excerpt out of a triangular lattice; **red:** Distance between nearest neighbours for simplicity set to 1; **pink:** Characteristic angle of $\frac{\pi}{3}$; **blue:** Visualization of the six bonds connecting a spin-site to its nearest neighbours

This configuration of lattice sites in equilateral triangles leads to the interesting phenomenon of geometrical frustration for the antiferromagnetic Ising coupling even in the nearest-neighbour model. Geometrical frustration occurs if the antiferromagnetic condition cannot be fulfilled for all bonds. That means regarding classical spin models, not all nearest neighbours of every lattice site can have a spin pointing in the opposite direction when the system is in the ground state. Thus the spin direction for several lattice sites is undetermined which leads to an extensive degeneration of the ground state. Figure 2 illustrates the geometrical frustration of spin-$\frac{1}{2}$ lattice-sites due to the antiferromagnetic condition.
This variety and degeneration of the ground state is one of the main reasons to study triangular structures. The extension to long-range coupling enhances the frustration of the system because just like the nearest-neighbour case the long-range couplings have to fulfil the antiferromagnetic condition to reduce the energy of the whole sys-

tem. This enlargement of conditions can lead to a reduction of the ground-state degeneracy, as we will see in the results of this thesis.

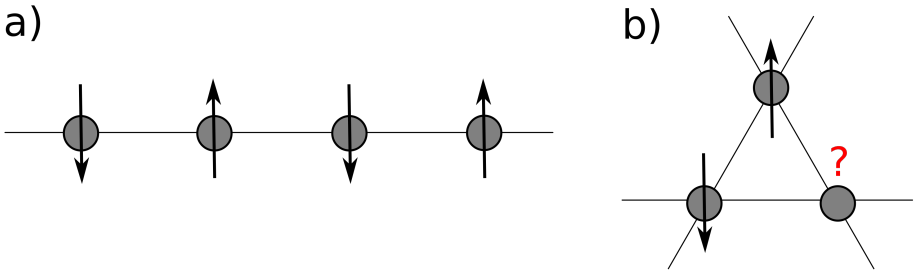

Figure 2: Illustration of geometrical frustration of antiferromagnetic coupling (nearest-neighbour case). **a) 1D spin-chain:** No frustration; if one fixes the spin-sign of one lattice site, one determines the whole ground state of the system. **b) 2D triangular lattice:** Geometrical frustration

2.2.2 Defining the YC(n)-lattice

We will now generalise the YC(6) structure described in paper [2] to an infinite cylinder with $n \in \mathbb{N}$ spin-sites on the circumference, by adding periodic boundary conditions in one lattice direction after n lattice-sites of the triangular lattice. As an example, the YC(4) lattice is visualised in figure 3.

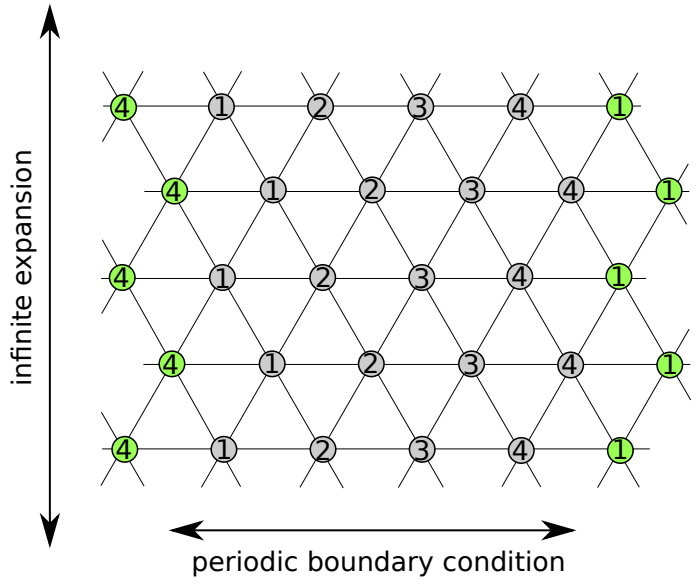

Figure 3: Illustration of the YC(4)-lattice

By adding the boundary condition like in figure 3, the dimension of the whole system is reduced from two to one, because it is no longer infinitely extended in two dimensions. This affects the possible coupling power-law exponent, which could now be $\alpha \in]1, \infty[$ without having any problems with the convergence of the series that describes the energy per spin-site. This one-dimensionality is also one reason to formulate an effective spin-chain model for the whole system.

It is now useful to divide the cylinder into the rings, the natural unit cells of YC(n)-lattices. One ring of the YC(n)-structure is made of n spin-sites in the direction of the periodic boundary. That means one horizontal slice of the lattice in figure 3. It is now the approach in this thesis to solve the Hamiltonian on one ring and introduce the coupling between rings perturbatively.
One can now discuss which properties of the 2D triangular lattice are inherited to the YC(n)-lattice. At first one can easily see that frustration is still present on the cylinder because the equilateral triangles are still the basic structure of the lattice. To reduce the ground-state degeneracy of a single ring of the cylinder, only even n are regarded. This is a necessary step because we will approach the ground state of the whole system by connecting the ground states of the rings. Therefore it is useful to have a small ground-state degeneracy on one ring, and in the best way always a twofold degeneracy to map the system on an effective spin-$\frac{1}{2}$ model. This is the case for even n.
For large n the cylinder shall behave like a normal 2D triangular lattice because the periodicity is less relevant due to bigger distances. But one should always be aware that only a small irregularity in the lattice structure, e. g. by the periodical boundary conditions or finite size effects can lead to new ordering phenomena. This is impressively shown in Shokef's and Lubensky's research on how irregularities in the geometrical symmetry of the triangular lattice affect the degeneracy of the ground state of the zero-field nearest-neighbour Ising model described in the following chapter [11].
At least the current research results described in the following chapter indicate, that if a ground-state phase in 2D shows a periodicity and this periodicity fits on the cylinder in every direction, it is very likely to also find this phase on the YC(n) structure.

2.3 Degenerate perturbation theory

In the following there will be a brief summary of ground-state perturbation theory introduced by Takahashi in [12] for Hamiltonians that consist of a unperturbed operator H_0 with a m-fold degenerate ground state and a perturbation V with perturbation parameter λ in the following way,

$$H = H_0 + \lambda V. \tag{4}$$

The ground state of H_0 with energy E_0 is m-fold degenerate, therefore one can introduce the space spanned by those eigenstates as U_0 and the projection Operator on that eigenspace as P_0. One can also define the space of perturbated eigenvectors from U_0 as U and the projector on that space as P. The explicit form of P results out of a resolvent contour Integral which leads to the following statement,

$$P = P_0 - \sum_{n=1}^{\infty} \lambda^n \sum_{k_1+k_2+...+k_{n+1}=n;\ 0\leq k_i} S^{k_1} V S^{k_2} V ... V S^{k_n} \tag{5}$$

with $S^0 = -P_0$ and $S^k = [(1-P_0)/(E_0 - H_0)]^k$ for $k \geq 1$ [13][14].
It is possible to consider a transformation from a vector $\phi \in U_0$ to a vector $\psi \in U$ by $\psi = \Gamma\phi$ using $\Gamma = PP_0(P_0PP_0)^{(-1/2)}$ [12] with,

$$(P_0PP_0)^{(-1/2)} = P_0 + \sum_{n=1}^{\infty} \frac{(2n-1)!!}{(2n)!!}[P_0(P_0 - P)P_0]^n. \tag{6}$$

This reduces according to Takahashi the eigenvalue problem $(H - E)\psi = 0$ to

$$(h - E)\phi = 0 \quad \text{with} \quad h \equiv \Gamma H \Gamma. \tag{7}$$

Using equation 7 one can expand h in orders of λ,

$$h = P_0 H_0 P_0 + \lambda P_0 V P_0 + P_0 V S V P_0 + \mathcal{O}(\lambda^3) \tag{8}$$

to evaluate h up to a certain perturbation order [12]. The terms that have to be evaluated for λ^n with $n > 2$ have the following form $P_0 V S^{k_1} V S^{k_2} ... S^{k_{n-1}} V P_0$ with prefactors out of $\mathbb{Q}$. The first and second-order expansion (equation 8) will be used in the investigation of the zero-field Ising model.
The great merit of Takahashi was the application of this perturbation scheme to the second quantization particle picture that we also use in quantum magnetism. Therefore one has to define the perturbation in a way of particle creating, annihilating and particle number preserving operators with respect to the zero-particle ground state of the unperturbed Hamiltonian. This picture makes it more easy to calculate the several orders. This approach will also be used in this thesis, the effective model for the low-field approach will be derived by high order ($\mathcal{O}(\lambda^{12})$) Takahashi's perturbation.

3 State of research

This chapter summarises the most important research results of the long-range but also the nearest-neighbour Ising model on the triangular and YC(6)-lattice to motivate the work done in this bachelor thesis. The other aim of this summary is the introduction of terminology to discuss this spin model properly and summarise the important findings for the reader.

3.1 2D triangular lattice Ising model

To describe the pure Ising model, one sets $h = 0$ in equation 3 that means no external field is applied. In this case, the Hamiltonian is diagonal

$$H = J \sum_{i>j} \frac{1}{|\delta_{i,j}|^{\alpha}} \sigma_i^z \sigma_j^z \ . \tag{9}$$

If only nearest-neighbour couplings are present the Hamiltonian is described by $\alpha = \infty$ and every state fulfilling the following condition is ground state of the system [9],

$$\prod_{\triangle} -\frac{J_{ij}}{J} = -1 \ . \tag{10}$$

That means every equilateral triangle unit cell consists of two spins having one sign and one of the opposite sign. This condition leads to the extensive degeneracy of the ground state. Already an infinitesimally small transverse field breaks this degeneracy, as described in the following section. It is interesting to mention that Shokef and Lubensky studied the nearest-neighbour zero-field Ising case on an asymmetric triangular lattice and found stripe-shaped structures like the ones discussed in chapter 5.3 (see figures 12 and 13 [11]).

Concerning the ground state of a further-neighbour coupling zero-field Ising model results are given by Korshunov in [15] and Smerald, Korshunov and Mila in [16] who used an artificially tuned coupling pattern for different coupling distances. The authors also found stripe structures for the zero-field case which were reproduced with the code used in this thesis.
In the zero-field long-range case, the antiferromagnetic conditions on different distances compete against each other, and the ground state is the energetically lowest combination. It is a natural assumption that the ground-state solution should be homogeneous for every lattice-site because the pure Ising coupling has no preferred direction. Hence translation symmetry should be obtained in the ground state.
At the end of the studies of the pure Ising model, a proposition of a possible 2D zero-field Ising ground state will be derived by expanding the YC(n) structure to large n.

3.2 2D triangular lattice transverse-field Ising model

The transverse-field nearest-neighbour Ising Hamiltonian (equation 2) applied on the 2D triangular lattice seems to be already well researched. In case of zero field, the nearest-neighbour model shows the highly-degenerated ground state described in the previous section. By applying a transverse field, the quantum fluctuations of this field induce an "order by disorder" phenomenon which results in a so-called clock order which is also sometimes called $\sqrt{3} \times \sqrt{3}$-order [2][8][9]. Regarding the particle picture used e. g. in Takahashi's expansion, quantum fluctuation means the creation or destruction of particles by the σ^x term of the field. The explanation of "order by disorder" is that this particle creation disturbs the ground state and leads to a reconfiguration of the ordering to a more stable phase.

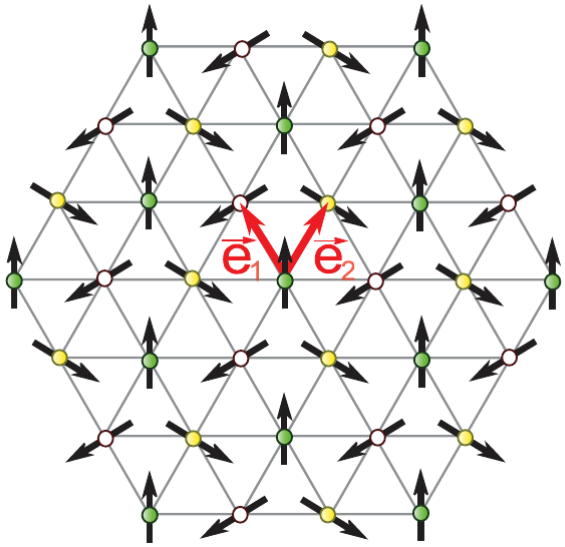

Figure 4: Illustration of the complex phase of the eigenstate corresponding to the one-particle gap at $\vec{k}_{\min} = (\frac{2}{3}\pi, -\frac{2}{3}\pi)$ in the high-field polarised phase. This exhibits a $\sqrt{3} \times \sqrt{3}$ structure. It has to be stressed that in this figure the arrows do not visualise spins[8].

The essence of the $\sqrt{3} \times \sqrt{3}$ phase is well described by summarising the results of Powalski, Coester, Moessner and Schmidt who approached this phase by analysing the the one-particle gap of the dispersion relation $\Delta^{\mathrm{tr}} = \omega^{\mathrm{tr}}(\vec{k}_{\min})$ perturbatively about the high-field limit [8]. With the aid of perturbative continuous unitary transformations, the authors calculated the one-particle gap up to eleventh order and found a periodical order for the complex phase of the eigenstate corresponding to the one-particle gap shown in figure 4 [8].
For increasing field strength, there is a second-order phase transition to the polarised phase in which the field term of equation 2 is dominating and polarising the spins in the anti-parallel direction to the field [8][9]. This phase transition can be characterised as a 3D-XY universality class phase transition, by regarding the critical exponents [9][8][10].

The 2D triangular lattice with transverse-field long-range interactions is subject of current research. Fey, Kapfer and Schmidt present promising results [3]. They used

perturbative continuous unitary transformations and classical Monte-Carlo methods to extract high-order series for the one-particle excitations in a high-field quantum paramagnet to investigate the breakdown of the polarised phase as a function of α [3]. With that they were able to evaluate the critical exponents of the system and confirm a phase transition between a $\sqrt{3} \times \sqrt{3}$-clock ordered phase and a polarised phase for coupling decay exponents α down to $\alpha \approx 2.5$. For smaller decay exponents the series to evaluate the one-particle excitations was no longer convergent and because of that no precise statements for the ground state in the low α limit could be formulated [3]. No indications of the stripe phases were found [17].

3.3 YC(6)-lattice transverse-field Ising model

In the following section the discoveries of Saadatmand, Bartlett and McCulloch [2] will be discussed in detail. At first we will present their results on the nearest-neighbour model, then their findings for the long-range interaction.
The authors find three different ground-state phases for the nearest-neighbour Ising model on the YC(6)-lattice. At $\frac{h}{J} = 0$ they find the classical highly-degenerate ground state of the pure Ising model that is also found on the regular 2D triangular lattice. If one applies a small field $0 < \frac{h}{j} \leq 0.75$ in addition to the pure Ising coupling, the quantum fluctuations induced by this external transverse field lead to the "order by disorder" effect. According to the authors of the paper these fluctuations lead to the clock-order described in the previous chapter. It should be stressed that this clock order could only exist on an YC(n)-lattice if $n = 3 \times m$ with $m \in \mathbb{N}$. That means the clock-order has to fit on the cylinder in every direction. The last phase described in [2] for the nearest-neighbour model is an x-polarised ferromagnetic order for $\frac{h}{j} > 0.75$ with a second order phase transition between the clock order and the x-polarised phase. This phase-transition could be classified with the 3D-XY [2] or the 2D-XY universality class, depending on whether the open boundary condition in one direction is within the relevant scale or not. In the x-polarised phase the field term of the Hamilton operator 2 is the dominant part, therefore the spins orientate themselves in anti-parallel field direction because of energy minimisation in the ground state.
The characteristics of the long-range interactions are best summarised by figure 5 published in [2]. The figure shows a phase diagram with different values of α and $\Gamma = \frac{h}{J} > 0.1$. For a high transverse field the system is in the x-polarised ferromagnetic phase like in the nearest-neighbour model. This x-polarised phase is achieved at different Γ-values for different coupling decay exponents α. In the limit of $\alpha \to \infty$ we expect the same phase transition behaviour like for the nearest-neighbour model for the phase transition between the clock-ordered phase and the x-polarised phase. As already mentioned for lower fields the authors of paper [2] find the "order by disorder"-induced clock order for high values of α and a columnar antiferromagnetic order for small α. The name columnar is chosen by the authors because there are columns of ferromagnetic order in the direction of the infinite extension of the cylinder. One can visualise the columnar phase they found by regarding figure 3 and considering every lattice-site that has the same ring-position (for example 1) being ferromagnetically coupled to each other and antiferromagnetically coupled with the stripes next to them. It has to be stressed that the columns proposed in [2] are not the ones that were found in this thesis by regarding the zero-field Ising ground

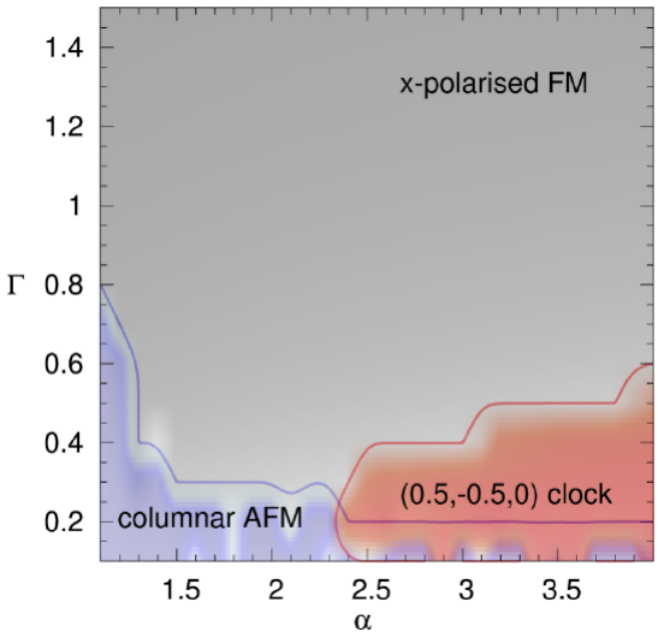

Figure 5: Phase diagram of the transverse-field long-range Ising model on the YC(6)-lattice [2]. α is the long-range coupling decay exponent and $\Gamma = \frac{h}{J}$ the magnetic field in units of J.

state of the YC(6) structure and a small-field perturbation in second order. This is most likely an artefact of the unit cell chosen the iDMRG by Saadatmand, Bartlett and McCulloch [18]. There are no explicit statements found on the pure long-range zero-field case of the YC(6) structure. But the results made in [16] could also be applied on YC(n)-lattices because the coupling distances they chose are present on every YC(n)-lattice with $n > 4$.
The existing results on the YC(6) structure are not contradictory to the findings on the 2D lattice. This is because in 2D the small values of α could not be described by the method used in [3]. Therefore the main point of interest should be to understand the columns on the cylinder and the mechanism leading to this stripe creation and then try to find general statements also for 2D.

4 Numerical and computational aspects

Nearly all results in this thesis were obtained by numeric means. This is due to the large 2^N-dimensional Hilbert space (N the number of spin-sites) for a spin-$\frac{1}{2}$ system. Although one could split up this large system using symmetry operations, even the transverse-field long-range Ising Hamiltonian (equation 3) on a ring of the YC(4)-lattice can not be solved analytically.
The main computations to evaluate matrix elements of the Hamiltonian were done using the script-language Python[1], because of the great opportunities of matrix operations by using the scientific packages NumPy[2] and SciPy[3].
The primary goal of calculations is the evaluation of matrix elements to get the matrix representation of the Hamiltonian. For small-size systems, one can easily derive the Hamiltonian directly by expanding the Pauli matrices with the Kroneckerproduct to the size of the Hilbert space and doing simple matrix multiplication and summation. It is also possible to evaluate the matrix elements directly by considering the scalar product $\langle a| H |b\rangle$ for which the Hamiltonian is simply evaluated. We would now like to introduce the two most important functions of the calculations in this thesis, at first the creation and representation of states, at second the distance-decay function $\frac{1}{|\delta_{i,j,R,R'}|^\alpha}$ in equation 13. The variables of these two functions include the complete information about the lattice and the state of the system.

4.1 State generation and representation

As already mentioned, the Hilbert-space of a finite spin-$\frac{1}{2}$ system has dimension 2^N. This combinatoric fact is used numerically to associate binary numbers $b < 2^N$ with the different states in a simple way. The 2^N combinations of spin-up/spin-down are represented by counting the binary numbers from 0 to $2^N - 1$ and associating each 1 with a spin-up and each 0 with a spin-down. These numbers are then converted in the python data-type list to make it easier to address a certain spin-site and combine different Hilbert spaces or make superpositions of these states. Superpositions of this "basic"-states could be done by storing the amplitude information and the different states in a list.

$N_{\text{spin-sites}}$	Number	Binary number	State
4	0	0000	|↓↓↓↓>
4	5	0101	|↓↑↓↑>
6	47	110001	|↑↑↓↓↓↑>

Figure 6: Example of the conversion of numbers to real-space spin representations

That approach is useful because it supports the separation of the YC(n)-lattice in several rings naturally and also supports the reconstruction of the whole system out of single rings. That is possible because one can gain the state of a whole system by just adding the components of it with the "+"-operator to each other what provides an easy and fast conversion of one state. One can find the code of the state generation in the appendix A.

[1] https://www.python.org/
[2] http://www.numpy.org/
[3] https://www.scipy.org/

4.2 Implementation of the YC(n)-lattice

The most important numerical task is the implementation of a functional YC(n) structure. In this approach the whole lattice information is stored in the distance-decay function $\frac{j}{|\delta_{i,j,R,R'}|^{\alpha}}$, which is already realised in the language of rings and positions the one ring. The function takes the following variables: number of spin-sites per ring, position on ring 1, position on ring 2, "number" of ring 1, the distance between the rings. By the term "number" of the ring it is meant, that for the implementation of the YC(n)-lattice in this form, it is necessary to define one ring as ring zero to address the single spin-sites by their positions on the ring and the ring-number. Therefore w. l. o. g. one ring is defined as ring zero. It is also implicitly assumed that the rings with odd numbers are the ones that are shifted to the right by $\frac{1}{2}$. All these features are shown exemplary for the YC4-lattice in figure 7.

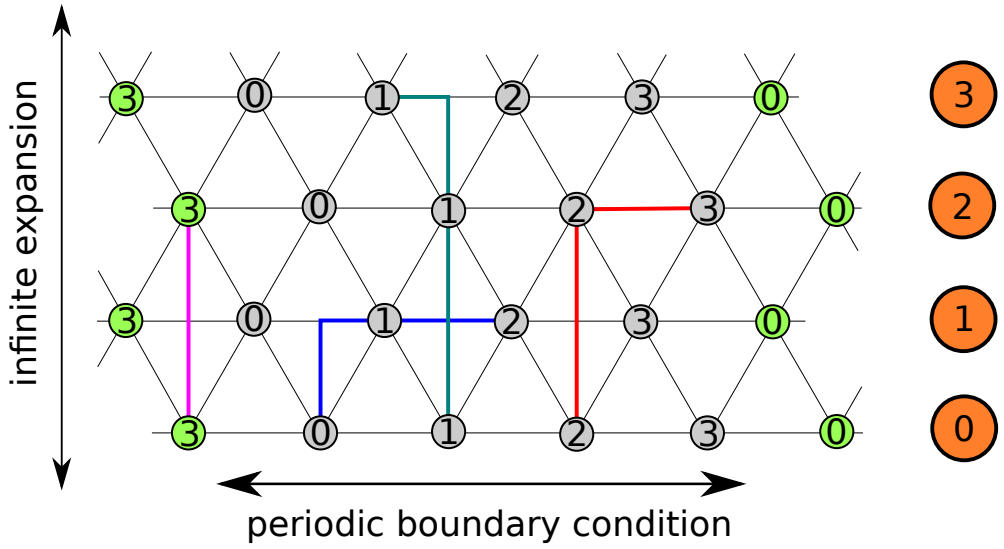

Figure 7: Illustration of the distance measurement on the YC(4)-lattice by using the theorem of Pythagoras. **Grey circles:** Positions on the ring; **orange circles:** Ring numbers; **green circles:** Illustration of the periodic boundary; **coloured paths:** Indicate the cathetes used for the Pythagoras theorem.

The evaluation of the distances is based on the Pythagoras theorem. One uses the distance between the rings and the distance in periodic boundary direction. The distance between the ring is a direct input variable, the distance in periodic boundary direction is determined by the positions on each ring and the ring-numbers of ring 1 and 2. The full code can be found in the appendix B.

5 Zero-field long-range Ising model on the YC(n)-lattice

As already mentioned, the first model that is investigated is the pure Ising Hamiltonian described in equation 9. After evaluating the ground state of this Hamiltonian on the YC(n) structure under certain assumptions, it will be checked whether this ground state is stable under quantum fluctuations by adding the local spin-flip field term in second order perturbation theory.

5.1 Ground state of a single ring

As described in chapter 2.2.2 where the YC(n) structure is introduced, one horizontal slice of the YC(n)-lattice is called a ring (see fig. 3). We call it a ring because it is an equidistant spin-chain with periodic boundary conditions. The lattice constant is set to one. Therefore the distance between two spin-sites in one ring is also one.

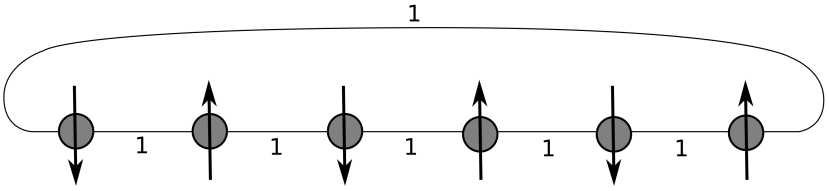

Figure 8: One ring of the YC(6)-lattice with outlined bond distances between the spin-sites. The arrows show one of the two possible ground states of the zero-field long-range Ising model for all $\alpha > 0$ on the ring.

The chosen approach to gain the ground state of the whole system for finite α is the construction by using the ground states of each ring and stacking them to a large finite YC(n) structure. It is not possible to create the ground state of the nearest-neighbour coupling in this way. We will show later on, that the ground state created in that way is the state with the lowest possible energy at finite α that fulfils the antiferromagnetic condition of the nearest-neighbour model described in equation 10.
Because the ground-state space of one ring is essential for the further investigation, it is useful to chose n in a way that the degeneracy of the ground state is as low as possible. For one YC(n)-ring the Hamiltonian 9 reduces to the following term,

$$H_R = \sum_{\substack{i>j \\ i,j=1}}^{n} \frac{1}{|\delta_{i,j}|^\alpha} \sigma_i^z \sigma_i^z \quad \text{with} \quad \delta_{i,j} = \begin{cases} i-j & \text{if } \; i-j \leq \frac{n}{2} \\ n-(i-j) & \text{if } \; i-j > \frac{n}{2} \end{cases} \quad . \tag{11}$$

One can now directly evaluate the diagonal matrix representation of this Hamiltonian either by summation over the Pauli matrices or by calculating the diagonal matrix elements for all eigenstates of the ring. These eigenstates are all 2^n combinations of spin-up and spin-down on the spin-sites. By looking at the evaluated matrix, one can directly see that the Hamiltonian fulfils the C_n-symmetry and the spin-flip symmetry. Therefore all eigenvalues corresponding to eigenvectors which only differ in rotation and spin-flip are equal.
One can now also determine the ground state of one ring by directly reading off

the lowest eigenvalues of the matrix. This leads to the following statements about the degeneracy of the ground state. In the case of an even n, the ground state is twofold degenerate and is described in the natural basis chosen above as alternation of one spin-site containing an up-spin and one spin-site containing a down-spin. The twofold degeneracy is due to the symmetry of the Hamiltonian. If n is odd, the degeneracy rises to $2 \times n$ because the ground state described for the even case does not fit on this ring. That is why every ground state of the odd ring consists of two neighbouring spins pointing in the same direction while the other ones alternate as in the even case. This ground state is n-times degenerate due to the rotation symmetry and on top of that two times degenerate due to the spin-flip symmetry.

n	ground states
3	$\|\uparrow\downarrow\downarrow\rangle$, $\|\downarrow\uparrow\downarrow\rangle$, $\|\downarrow\downarrow\uparrow\rangle$, $\|\downarrow\uparrow\uparrow\rangle$, $\|\uparrow\downarrow\uparrow\rangle$, $\|\uparrow\uparrow\downarrow\rangle$
4	$\|\uparrow\downarrow\uparrow\downarrow\rangle$, $\|\downarrow\uparrow\downarrow\uparrow\rangle$
5	$\|\uparrow\uparrow\downarrow\uparrow\downarrow\rangle$, ... all 5 rotations + spin-flips
6	$\|\uparrow\downarrow\uparrow\downarrow\uparrow\downarrow\rangle$, $\|\downarrow\uparrow\downarrow\uparrow\downarrow\uparrow\rangle$

Figure 9: Ground states of one ring for small n

For further investigations we will only regard even n because it allows a natural low-energy description in terms of effective pseudo spins. Apart from the degeneracy of the ground state, the energy gap between the ground state and the first excited state is a point of interest. This has several reasons: At first a gap between the ground state and the first excited state makes it possible to consider the ground state as separated from the excited states and derive an effective model by labelling the two ground states with pseudo spins like we will do later on. The other reason is that if the ground states are separated by a large gap from the excited states, this will support the assumption that when the whole cylinder is in the ground state every ring is in its ground state because the energy of the coupling between rings is not high enough to compensate the energy gap for one ring.

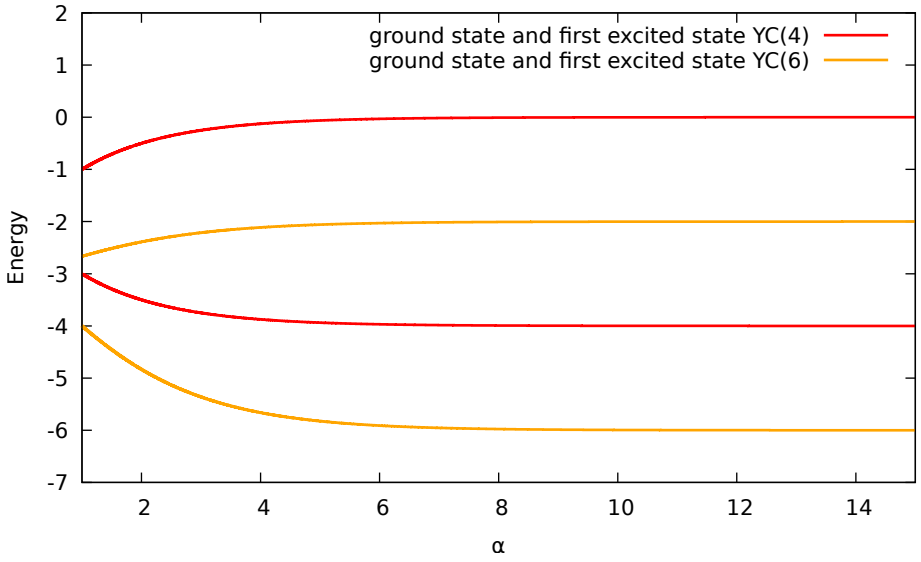

Figure 10: Illustration of the gap between the ground state and the first excited state

In figure 10 there is a plot of the ground-state energy depending on α. The first important thing to notice in that figure is that the gap between the ground state and the first excited state could always be assumed as big, at least for the YC(4) and YC(6)-lattice which are mainly analysed. However, one can also see, that the gap decreases for small α with rising n. Hence generalisations to 2D systems for small alpha should be treated with care.
For the further numerical investigation, it will always be checked that the ground state of one ring has the assumed form and degeneracy.

5.2 Perturbative introduction of coupling between rings

The coupling between the rings is introduced perturbatively by separating the Hamiltonian of the whole YC(n)-lattice in the following way,

$$H = J \sum_{R,R'=-\infty}^{\infty} \sum_{\substack{i,j=1 \\ (i,R)\neq(j,R')}}^{n} \frac{1}{|\delta_{i,j,R,R'}|^{\alpha}} \sigma^z_{i,R}\sigma^z_{j,R'} \tag{12}$$

$$H = \underbrace{J \sum_{\tilde{R}=-\infty}^{\infty} \sum_{\substack{i>j \\ i,j=1}}^{n} \frac{1}{|\delta_{i,j}|^{\alpha}} \sigma^z_{i,\tilde{R}}\sigma^z_{j,\tilde{R}}}_{H_0} + \underbrace{J \sum_{\substack{R>R' \\ R,R'=-\infty}}^{\infty} \sum_{i,j=1}^{n} \frac{1}{|\delta_{i,j,R,R'}|^{\alpha}} \sigma^z_{i,R}\sigma^z_{j,R'}}_{V} \tag{13}$$

in the coupling between spin-sites of one ring and the coupling between the spin-sites of different rings. The first summation is over the rings with R, R' as indices addressing them. The second summation is over the spin-sites of one ring which are addressed by i and j. $\frac{1}{|\delta_{i,j,R,R'}|^{\alpha}}$ denotes the algebraic decay function for the coupling. One can now identify the first sum as an unperturbated Hamiltonian H_0 which only depends on the state of the different rings and a perturbation V taking the coupling between the rings into account,

$$H = H_0 + \lambda V. \tag{14}$$

We introduce the perturbation parameter $\lambda \in [0, 1]$ which regulates the coupling between the rings relative to the coupling in one ring. For $\lambda = 0$ one gets decoupled rings, for $\lambda = 1$ the full Hamiltonian of the YC(n) system is restored.

The great benefit of this separation is the reduction of summation processes necessary to evaluate the matrix elements for a finite YC(n) structure. That is because H_0 always provides a certain eigenvalue of one ring depending on the state of the evaluated ring. So one only has to evaluate the coupling between rings. If we make the assumption that the ground state of the total YC(n)-lattice consists only of rings in their ground state, then the evaluation reduces even more because H_0 is then just $\sum_R e_0$ a sum over the ground-state energy of one ring. It is for practical reasons beneficial to normalise that sum and the whole matrix elements later with the number of spin-sites to gain the energy per spin-site, a quantity that is much handier and comparable than the extensive total energy of a finite system. Hence H_0 always gives the same result. The crucial point is the coupling between the rings that means the sequence in which the two different ground states of the ring are ordered.

In this case the first order perturbation reproduces already the exact Hamiltonian H. First one has to notice that V is diagonal in the eigenbasis of H_0. Therefore every operation of V on the space spanned by the ground states of H_0 does not leave this space. If one now looks at equation 8 and the higher orders in λ, they all consist out of terms containing multiples of $S = (1 - P_0)/(E_0 - H_0)$ like $P_0 V S^{k_1} V ... V S^{k_{n-1}} V P_0$. Now if one acts with such an operator on a state one will first project on the ground-state space with P_0, then the application of V would not leave the ground-state space. Hence the $(1 - P_0)$ in every S will project everything out of that space, what makes every order higher than $\mathcal{O}(\lambda^1)$ vanish. In the next section we will see that the long-range coupling will lead to a ferromagnetic stripe formation in the infinite direction of the cylinder and it will be determined which kind of stripes is favoured on what cylinder.

5.3 Ground state evaluation on a large finite YC(n)-lattice

We assume that the ground state of the whole system depends on the sequence of the two different ground states of one ring. If one evaluates the coupling between two rings being in the ground state for different α, one can directly see the first feature of the system. Two rings in the ground state which have an odd ring-distance could not be coupled. That means for matrix elements which describe a coupling between these rings being in ground state (GS),

$$\langle \text{GS Ring 1}| \otimes \langle \text{GS Ring 2}| \quad \lambda V \quad |\text{GS Ring 1}\rangle \otimes |\text{GS Ring 2}\rangle = 0 \tag{15}$$

if the ring-number difference is odd and one takes the ground states of figure 9. This results from the fact that every spin-site of ring 1 is coupled with two corresponding spin-sites on ring 2 which have the same distance, but the Pauli matrices acting on the ground states provide a different sign. This is independent of the choice which of the two ground states is on ring 1 and ring 2.

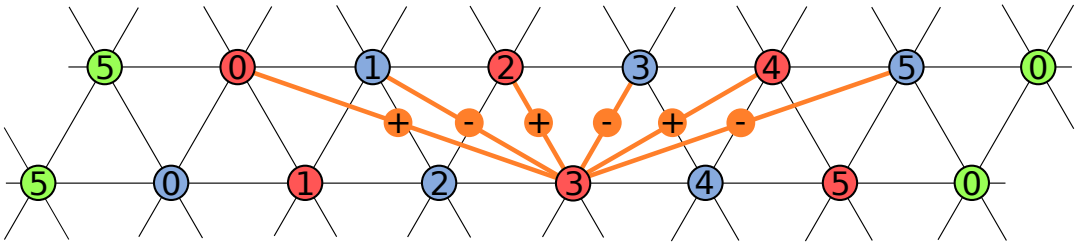

Figure 11: Depiction of the coupling between two rings in the ground state with ring distance 1. **Red circles:** Spin-sites with spin-up; **blue circles:** Spin-sites with spin-down; **green circles:** Periodic boundary conditions; **orange lines:** Distances with the sign due to the evaluation of the Pauli matrices on the spin-sites they are connecting.

Regarding the whole system the amount of calculations that have to be done reduces therefore even more because only Ising couplings between rings of even distances are not vanishing. This is because they do not have this property that two distances with opposite sign make their contribution vanish. That makes the whole problem split in two sub-lattices.

The next step is the ground-state investigation of systems of 10-15 rings with open and periodic boundary conditions and finding the energetically lowest ordering patterns according to different YC(n)-lattices and decay-exponents α. Therefore one tries all different combinations of rings in the two ground states.
For $n = 4 \times m$ with $m \in \mathbb{N}$ we find two different energetically beneficial configuration patterns with a first-order phase transition between them at a certain α_c, depending on n. We will later see in the quantitative calculations on a larger number of rings that $\alpha_c < 1$ if $n > 32$. For $\alpha < \alpha_c$ the coupling between the rings with even distances is minimised if they are in the same ground state. This results in a zigzag-stripe phase (see fig. 12). There are four different combinations to distribute the two ground states of one ring on the even- and odd-numbered rings which leads to that four-fold degeneracy. This can be understood in the following way: If all even rings are in the same ground state (e. g. $|\uparrow\downarrow\uparrow\downarrow\rangle$ for the YC(4)) then the odd rings have two possibilities, either being in the same state or the other ground state. If one then uses the spin-flip symmetry this leads to the four-fold degeneracy, which can be seen in figure 12.

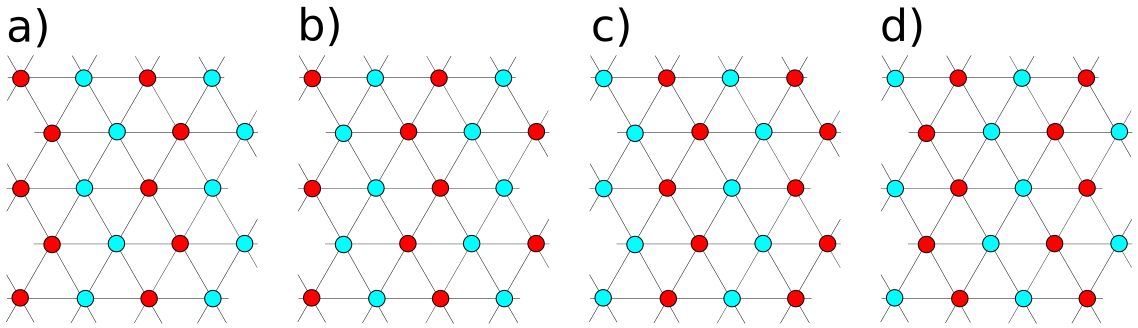

Figure 12: Excerpt of a YC(n)-lattice showing the zigzag-stripe state. Red circles represent spin-up lattice-sites, blue circles spin-downs. **a):** Zigzag-stripe state with same ground state even and odd numbered rings; **b):** Zigzag-stripe state with opposite ground state on even and odd-numbered rings; **c):** Spin-flip symmetrical state of a); **d):** Spin-flip symmetrical state of b);

If one looks at the energetically most beneficial order for $\alpha > \alpha_c$ one receives a different order for the lowest energy. In this case, the coupling between the rings with even distance is minimised if the ground state of the rings is alternating. That means if one ring is in a certain ground state, the rings with distance two should be in the opposite one. This leads to a four-fold degenerate plain-stripe state (see fig. 13). The degeneracy is due to the same arguments like in the zigzag order. One should stress that there is no difference in that behaviour depending on whether one chooses open or periodical boundary conditions, except the periodical case if the alternating order does not fit on the periodical torus, that means the number of rings is not a multiple of four.
The ground state depending on α of finite YC(n)-lattices considering n is not a multiple of four, shows a different behaviour. In this case there is no phase transition between different stripe types on the cylinder. Only the plain-stripe state is found for all algebraic decay exponents α.

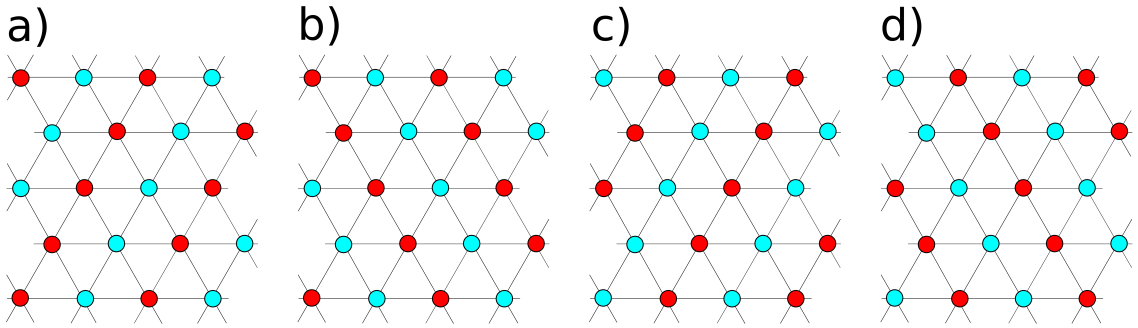

Figure 13: Excerpt of the YC(n)-lattice showing the plain-stripe state. Red circles represent spin-up lattice-sites, blue circles spin-downs. **a)-d):** fourfold degeneracy of the plain-stripe state;

That slightly different behaviour results from the different number of further neighbours and the sign of the couplings between them, plus the proportion between the different distances according to the decay exponent alpha. It will now be schematically demonstrated by regarding the YC(4)/YC(6)-lattice and the coupling between two rings with a ring-number difference of two how the two stripe states behave. Therefore we evaluate the zero-field long-range Ising coupling for one spin-site to all other spin-sites of the system as shown in figure 14.

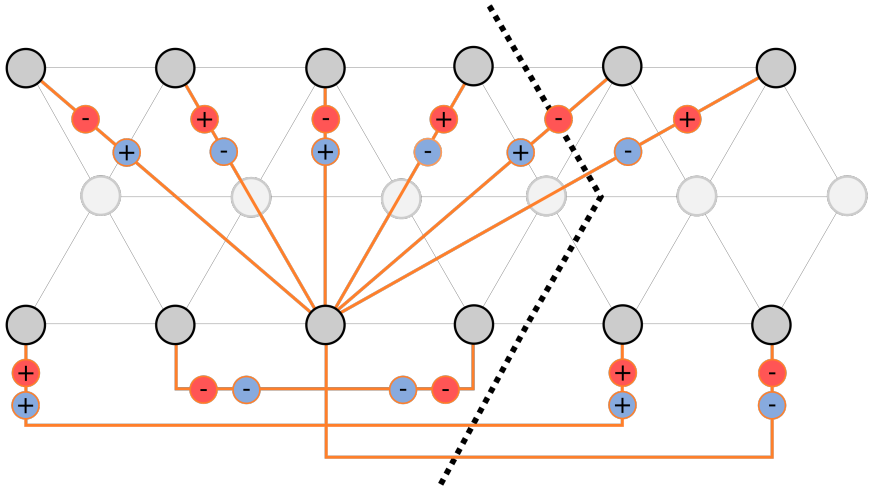

Figure 14: All Ising couplings of one spin-site in a system of two rings with a ring-number difference of two. **Red circles:** Sign of the coupling for the plain stripes; **blue circles:** Sign of the coupling for the zigzag stripes.

If one now evaluates the energy of the couplings of one spin-site with the others in the following form

$$e = \sum_i \frac{1}{|\delta_{0,i}|^\alpha} \cdot \mathrm{sgn}(m_0 \cdot m_i) \tag{16}$$

for the YC(4) and YC(6) lattice and the different stripe-states, one can understand which terms are important and how they differ between the different lattice types.

$$e_{\text{YC(4), zigzag}} = \underbrace{-2 + \frac{1}{2^\alpha}}_{\text{coupling on the ring}} \underbrace{+\frac{1}{\sqrt{3}^\alpha} - 2 \cdot \frac{1}{2^\alpha} + \frac{1}{\sqrt{7}^\alpha}}_{\text{coupling with the other ring}} \tag{17}$$

$$e_{\text{YC(4), plain}} = \underbrace{-2 + \frac{1}{2^\alpha}}_{\text{coupling on the ring}} \underbrace{-\frac{1}{\sqrt{3}^\alpha} + 2 \cdot \frac{1}{2^\alpha} - \frac{1}{\sqrt{7}^\alpha}}_{\text{coupling with the other ring}} \tag{18}$$

$$e_{\text{YC(6), zigzag}} = \underbrace{-2 + 2 \cdot \frac{1}{2^\alpha} - \frac{1}{3^\alpha}}_{\text{coupling on the ring}} \underbrace{+\frac{1}{\sqrt{3}^\alpha} - 2 \cdot \frac{1}{2^\alpha} + 2 \cdot \frac{1}{\sqrt{7}^\alpha} - \frac{1}{\sqrt{12}^\alpha}}_{\text{coupling with the other ring}} \tag{19}$$

$$e_{\text{YC(6), plain}} = \underbrace{-2 - 2 \cdot \frac{1}{2^\alpha} + \frac{1}{3^\alpha}}_{\text{coupling on the ring}} \underbrace{-\frac{1}{\sqrt{3}^\alpha} + 2 \cdot \frac{1}{2^\alpha} - 2 \cdot \frac{1}{\sqrt{7}^\alpha} + \frac{1}{\sqrt{12}^\alpha}}_{\text{coupling with the other ring}} \tag{20}$$

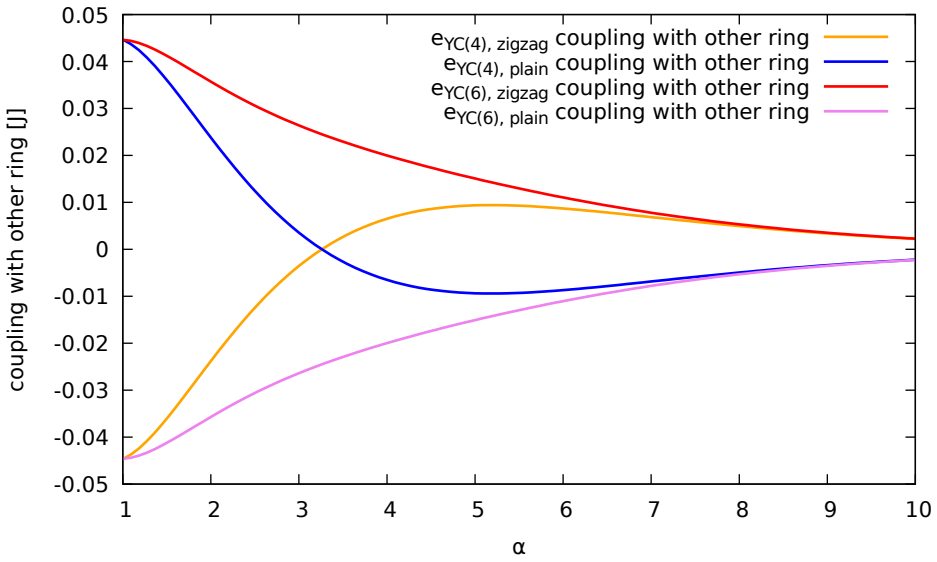

Figure 15: Comparison of the "coupling with the other ring" for the YC(4)/YC(6)-lattice and the plain and zigzag stripes. The excerpt of YC(4) lattice shows a change of order from zigzag to plain stripes at $\alpha \approx 3.3$. The excerpt of YC(6) structure always prefers the plain stripe order

The calculated energies above show, that the coupling on the ring of the lattice-site is always the same and therefore only the coupling with the other ring is important for determining which order is energetically beneficent. One can see directly, that the "coupling with the other ring" of the different stripes differs only by a factor of -1. In figure 15 one can see the energies as a function of α. One can see that the YC(4)/YC(6)-lattice excerpts behave like the larger systems. This shows impressively that even this smallest possible lattice excerpt shows the behaviour needed for the stripe phases. In principle figure 15 looks the same for YC(n)-structures with bigger n, according to whether n is a multiple of four or not. Trough, the crossing point between the different stripe-orders is at lower α.
After understanding that the two stripe formations are the energetically most beneficial order created out of the ground states of the individual rings, it is easily

possible to calculate the energy per spin-site of these two specific phases directly for large systems of 1000 rings that means $N_{\text{spin-site}} = 1000 \cdot n$ spin-sites with open boundary conditions to get a quantitative result for the different α_c and to see that this behaviour also remains close to the thermodynamical limit. This calculation is done by evaluating the following series with a summation over all spin-sites i, j,

$$\frac{E_{\text{zigzag}}}{N_{\text{spin-site}}} = \sum_{R \leq R'}^{1000} \sum_{i,j}^{n} \frac{1}{|\delta_{i,j,R,R'}|^{\alpha}} (-1)^{i+j} \tag{21}$$

$$\frac{E_{\text{plain}}}{N_{\text{spin-site}}} = \sum_{R \leq R'}^{1000} \sum_{i,j}^{n} \frac{1}{|\delta_{i,j,R,R'}|^{\alpha}} (-1^{i+j+\kappa}) \quad \begin{cases} \kappa = 1 & \text{if} \quad (R' - R) \bmod 4 = 2 \\ \kappa = 0 & \text{if} \quad (R' - R) \bmod 4 = 0 \end{cases} . \tag{22}$$

κ is defined by using the fact that only couplings between rings of even ring-number difference contribute. The other couplings of rings with odd ring-number difference vanish independently of κ, therefore it is not necessary to define κ in a more precise way to describe the plain stripes correctly.
By regarding even larger systems than 1000 rings for one particular α, one can see that the series is already well converged for 1000 rings. The difference of the energy per spin-site towards 10^6 rings, depends on α, and is of magnitude $10^5 J$ (small α), $10^6 J$ (big α). Hence 1000 rings is a good compromise between precision and computation time. The evaluation of the series is done by implementing them in C++ to improve the computation time.

YC(n)	ground-state phases	α_c
YC(4)	zigzag-stripe phase - plain-stripe phase	3.295 ± 0.005
YC(6)	plain-stripe phase	-
YC(8)	zigzag-stripe phase - plain-stripe phase	1.9 ± 0.005
YC(10)	plain-stripe phase	-
YC(24)	zigzag-stripe phase - plain-stripe phase	1.11 ± 0.005
YC(28)	zigzag-stripe phase - plain-stripe phase	1.045 ± 0.005
YC(32)	zigzag-stripe phase - plain-stripe phase	1.0 ± 0.005
YC(36)	plain-stripe phase	$\alpha_c < 1$

Figure 16: The table shows the results of the quantitative investigation of YC(n)-lattices with n being a multiple of four show the phase transition between zigzag and plain-stripe phase at a critical α_c. For $n > 32$ one we find $\alpha_c < 1$. In the case that n is not a multiple of four only the plain-stripe phase is found for all α.

The main results of this sum evaluation are summarised by the figures 16 and 17. Figure 16 shows the critical α, for the phase transition between the stripe phases when the YC(n)-lattices where n is a multiple of four. And the n from which on multiples and no multiples of four act in the same way. In figure 17 the global behaviour of the energy per spin-site is plotted for the YC(4), YC(6), YC(36) and YC(38)-lattice to illustrate the energetic trend of the orderings. One can also see that in the limit of $\alpha \to \infty$ both stripe configurations become equally beneficent at a energy per spin-site of $-J$. This is because both configurations fulfil the nearest-neighbour condition (see equation 10). In reverse that means the highly-degenerate ground state for $\alpha = \infty$, with every state fulfilling 10 being a ground state, reduces

its degeneracy for finite α to the four-fold degeneracy of the preferred stripe states. This statement was proven for finite lattices of 10-12 rings, by constructing all possible states that obey the nearest-neighbour condition and calculating their energy. By doing so one can formulate the assumptions made to evaluate the ground states even tighter.

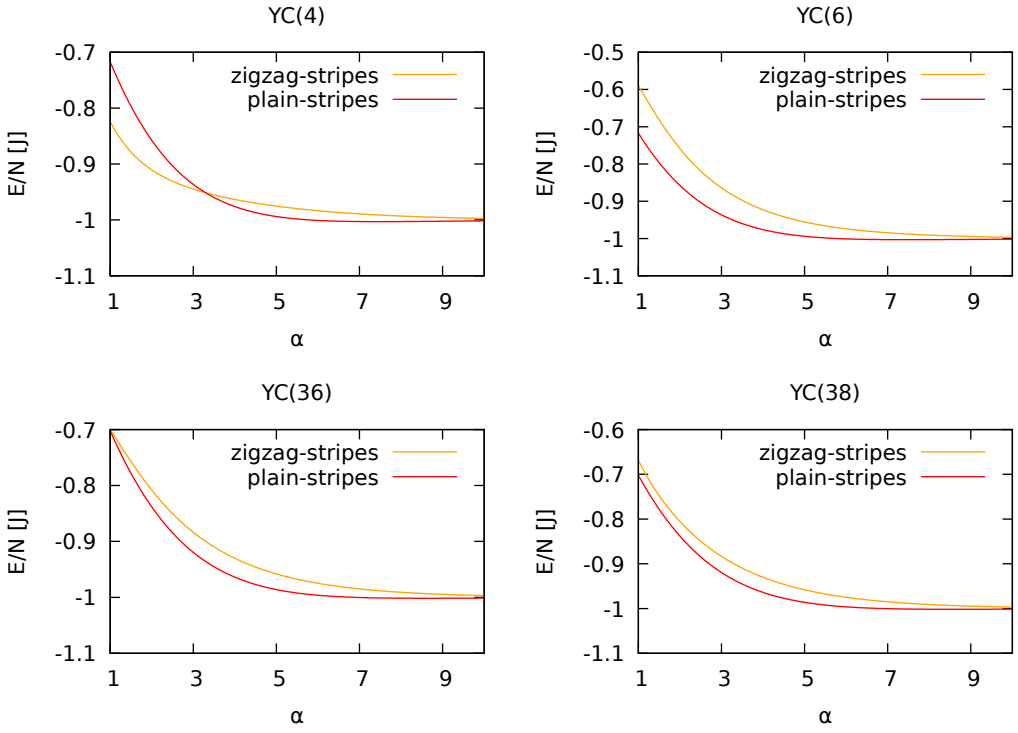

Figure 17: Energy per spin-site of the zigzag and plain-stripe phase for different YC(n) structures. For small n the difference between multiples and not multiples of four is decisive for the global behaviour. For $n > 32$ the behaviour is approximately the same.

The stripe ground states described in this thesis for the antiferromagnetic long-range Ising model are the energetically most beneficent configurations that can be constructed out of the ground states of one ring and also the energetically most beneficent state that is also ground state of the nearest-neighbour model. The stripe configurations are part of the ground-state space of the nearest-neighbour model. So it is possible to interpret the difference between the infinite and finite α in the following way: In the infinite case there is the extensively large ground-state space of all states obeying the condition 10 on the YC(n)-lattice. That infinite degeneracy reduces as soon as α becomes finite and the complete ground-state space reduces to the stripe phase. We deduce the following: If there is no further process that leads to another phase transition in the zero-field case involving other states than the ones in the $\alpha = \infty$ ground-state manifold, the stripe phases we have calculated are the actual ground states of the pure Ising model on the YC(n)-lattice. It must be stressed that there is no indication for any process that would lead to this behaviour.

5.4 Perturbation due to a small transverse field

After calculating the ground state of the zero-field Ising model for finite α it is now interesting to see how the stripe states behave under the application of a small transverse-field. This is motivated by the columnar phase described in reference [2], because if the stripe phases are stable under the application of a small transverse-field perturbation, this could underline the proposal of a columnar stripe order at finite field. This stability would also indicate that even for large finite α on the YC(n)-lattice, the application of a transverse field would not directly lead to the clock-order phase but that there is a range of h for which the zero-field ground-state phase stays stable.
To evaluate this fluctuation, we will introduce a small transverse-field perturbation on the zero-field long-range Ising Hamiltonian H_0 of the form,

$$H = H_0 + h\sum_i \sigma_i^x = H_0 + hV_{\text{field}} \tag{23}$$

and evaluate the ground-state energy of the stripe phases up to the second-order in h perturbatively as described in equation 8. In zeroth order $P_0H_0P_0$ the known ground-state enregy of the stripe phases is obtained. The first-order correction $hP_0V_{\text{field}}P_0$ vanishes because the application of the field on a stripe phase results in a state that is not in the space spanned by the ground states. Hence the second P_0 will project everything to zero. That makes the second-order the first non-trivial correction to the zero-field Ising model. The only non-zero contribution is the one in which both local perturbations V_{field} in $h^2P_0V_{\text{field}}SV_{\text{field}}P_0$ act on the same lattice-site because otherwise the same situation as described for the first-order term appears and the second projector makes the contribution disappear. The Hamiltonian H_0 is also translationally invariant in the direction of infinite extension and invariant under rotation and spin-flip on one ring. The following calculation is based on these considerations. The operators P_0 and $(1-P_0)$ will not be explicitly notated because the stripes are part of the ground-state subspace and every local excitation of that state will be in the subspace with projector $(1-P_0)$. Therefore the calculation of the matrix element reduces in the following way for stripe phases on the YC(n)-lattice

$$\langle\text{stripe}|\, V_{\text{field}}\frac{1}{E_0-H_0}V_{\text{field}}\,|\text{stripe}\rangle = h^2\sum_{i_1,i_2}\langle\text{stripe}|\,\sigma_{i_1}^x\frac{1}{E_0-H_0}\sigma_{i_2}^x\,|\text{stripe}\rangle =$$

$$= h^2\sum_i\langle\text{stripe}|\,\sigma_i^x\frac{1}{E_0-H_0}\sigma_i^x\,|\text{stripe}\rangle = \frac{N_{\text{spin-sites}}}{n}h^2\sum_\nu^n\langle\text{stripe}|\,\sigma_\nu^x\frac{1}{E_0-H_0}\sigma_\nu^x\,|\text{stripe}\rangle =$$

$$= N_{\text{spin-sites}}\cdot h^2\,\langle\text{stripe}|\,\frac{1}{E_0-H_0}\,|\text{stripe}\rangle = N_{\text{spin-sites}}\cdot h^2\frac{1}{\Delta E_{\text{excitation}}}\quad,$$

what results in the following corrected term for the ground-state energy per spin-site,

$$\frac{E}{N_{\text{spin-sites}}} = \frac{E_0}{N_{\text{spin-sites}}} + h^2\frac{1}{\Delta E_{\text{excitation}}}. \tag{24}$$

The correction $\frac{1}{\Delta E_{\text{excitation}}}$ is easy to evaluate because the only term which has to be calculated, $E_0 - E_{\text{one spin-site fliped}}$, is nothing but two times the energy of one excited spin-site coupled with all the other ones on the lattice. Only contributions, where the excited spin-site is involved, are not vanishing because they have the opposite

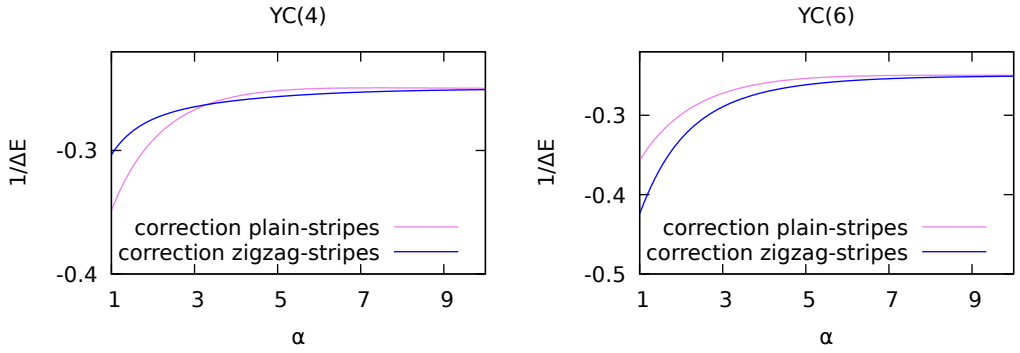

Figure 18: Correction $\frac{1}{\Delta E_{\text{excitation}}}$ of the zigzag and plain-stripe phase for different YC(n) structures. For small n the difference between multiples and no multiples of four is decisive for the global behaviour. For $n > 32$ the behaviour is approximately the same. One can nicely see that the energetically less beneficent state (fig. 17) is more lowered by the correction term.

sign in $E_{\text{one spin-site fliped}}$ than in E_0. Thus the field correction reduces the energetically less beneficial stripe configuration more.
The evaluated $\frac{1}{\Delta E_{\text{excitation}}}$ are presented in figure 18. They show in connection with 17 that the two stripe phases do not behave equally and that depending on the strength of the field different stripe formations could occur. One can now also compute the second-order corrected energy per spin-site for all (α, h) and compare which of the two discussed stripe types is energetically lower. The ground-state development in h could be nicely visualised in a "phase-diagram" of the two phases (see figure 19), that shows the expected behaviour.

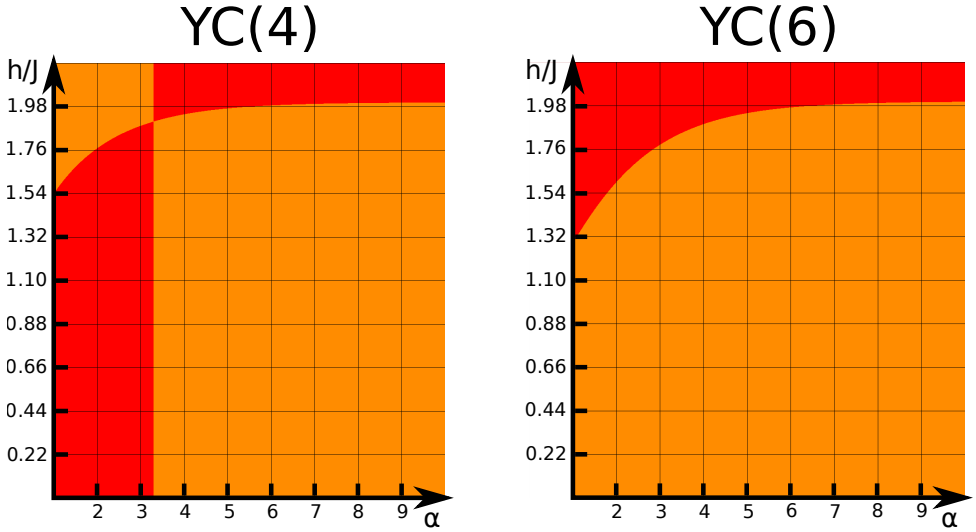

Figure 19: Diagrams that indicate which stripe formation is energetically more beneficial at a certain (α, h). **Red:** zigzag-stripes; **orange:** plain-stripes;

A quite large transverse field has to be applied to change the stripe type to the less beneficial one at $h = 0$, although both of them are part of the space spanned by a combination of zero-field Ising ground states of individual rings. Out of the construction of the two stripe phases one could interpret them as extrema of the cou-

pling behaviour of the second-nearest neighbour rings, with the plain stripe phase as an antiferromagnetic coupling with alternating ground states and the zigzag stripes as a ferromagnetic coupling. It can be argued that besides the two stripe-states described in figure 12 and 13 there could be "mixed"-configurations with domains of plain and zigzag stripes like Korshunov proposed for 2D triangular lattice, but required therefor a non-trivial phase transition between the stripe phases at zero field and a "rather special" relation between the coupling constants [15].
These mixed-phases would have an energy, depending on the proportions of the two stripe types, between the two pure stripe energies in the plots in figure 17. Hence their second order corrections $\frac{1}{\Delta E_{\text{Excitation}}}$ should be according to equation 24 for the stripe states and a continuous transition between the two stripe phases, between the corrections of the pure stripes in figure 18. Such phases were also investigated by Smerald, Korshunov and Mila in reference [16], who investigated relations between the coupling constants of the second-nearest and third-nearest neighbour spin-site couplings. The code used in this thesis was able to reproduce the zero-field results of their phase diagram on YC(n)-lattices with large n. Both references show generically at zero field a first-order phase transitions between the two stripe phases but at finite temperature with "special relations [15]" between J_2, J_3 and J_5 (J_n coupling with the n-th nearest neighbour) a nematic phase between the stripe phases triggered by the presence of the coupling of J_5. If this special relation is also included in the complete long range model indications of it should be found in the effective spin model. Hence the exploration of this variety of possible mixed states is one of the questions that motivate the effective model derived in the following chapter. One can already say in advance, that the effective model indicates that there are no mixed-stripe phases and these phase diagrams summarise the second-order low-field behaviour properly.

The perturbative investigation in this section showed that one needs a quite large field to change the state of the system from the preferred to the not preferred stripe order which are both build of ground states of individual rings. One can argue that to realise a clock order it is not enough to use the ground states of one ring but also the excited states. According to figure 7 an involvement of excited states for finite α always needs a certain amount of energy because configurations with these states on rings are not included in the ground-state space of the pure Ising model. Therefore in contrast to the nearest-neighbour Ising model on YC(n)-lattices we state that the zero-field ground-state space with the stripes as leading solutions is stable under field fluctuations.

5.5 Proposal for a 2D zero-field long-range Ising ground state

We investigated in figure 16 the behaviour of YC(n) structures with large n and found for $n > 32$ that the plain-stripe state is the ground state of the system for all α. Therefore we propose this configuration as a possible ground state of the zero-field Ising Hamiltonian on the 2D triangular lattice. It has to be stressed that this is only a proposal and it needs to be investigated how strong finite size effects due to the cylinder condition influence the generalisation to 2D. But the findings in reference [16] underline that some kind of stripe formation is also happening in 2D

for long-range interactions. Also the results of [11] could be seen as an indication of stripe phases in the long-range 2D case, because in their research the nearest-neighbour extensive ground-state degeneracy breaks due to an anisotropy of the lattice, inducing stripes. In our research the degeneracy of the nearest-neighbour case also breaks, but here due to a finite α. Hence it is likely that our breaking of the degeneracy leads to similar results.
In the following chapter we will return to the YC(n)-lattices and derive an effective model to gain more information about small transverse-field applications.

6 Effective 1D spin model

The primary motivation to look at an effective low-field limit model with rings as new pseudo spin-sites is the further investigation of small transverse-field perturbations and the possibility to find an indication of a $\sqrt{3} \times \sqrt{3}$-clock order. Until now we can conclude that the low-field approach is an excellent way to find the stripe phases, but it shows no indication of the clock order. The other point is the understanding of the stability of the stripe phase and a possible mixed-phase due to the quantum fluctuations induced by the transverse field. To derive a complete effective model for a long-range Ising Hamiltonian is very demanding and due to the complexity of the system and the time limitation to finish this thesis, the focus will lie on the quantitative description of the effective terms derived from small cluster sizes.

6.1 General setting

As we know the clock order already appears in the nearest-neighbour transverse-field Ising model on a YC(n)-lattice. Therefore it is the primary task to explore the coupling between two neighbour rings which does not occur in the zero-field case. Also, the binding distances needed for a hypothetical mixed-stripe phase should be included in the setting we will look at. Because of that, the system which is now explored by Takahashi's expansion consists of three rings with open boundary conditions. On the one hand, there is the coupling between the first and the third ring that has a ring number distance two which is the important coupling distance occurring in the stripe formations of the pure Ising model. On the other hand, the couplings between the first and the second ring or the second and the third ring are couplings between nearest neighbours on which a indication for clock ordering can be expected.
Now we denote the zero-field Ising Hamiltonian on each ring without coupling between the rings as H_0. We define the ground-state space of one ring as the zero-particle sector and the other excited states of one ring as the one-particle sector. As an example, we look at a YC(4) ring. If this ring is in a ground state, e. g. $|\uparrow\downarrow\uparrow\downarrow\rangle$, we say there is no particle on that super-site, but if this ring is not in ground state e.g. $|\uparrow\uparrow\uparrow\downarrow\rangle$ the super-site contains a particle. Hence every process that leads from a ground state to an excited state is a one-particle creation process, and the ones that transform excited states to ground states are particle annihilations.

$$H = H_0 + \frac{h}{J} V_{\text{field}} + \lambda_1 V_{\text{nearest Ring}} + \lambda_2 V_{\text{second n. Ring}} \tag{25}$$

$$H_0 = \sum_R \sum_{i>j} \frac{1}{|\delta_{i,j}|^\alpha} \sigma^z_{i,R} \sigma^z_{j,R} \tag{26}$$

$$V_{\text{field}} = \sum_R \sum_i \sigma^x_{i,R} \tag{27}$$

$$V_{\text{nearest Ring}} = \sum_R \sum_{i,j} \frac{1}{|\delta_{i,j,R,R+1}|^\alpha} \sigma^z_{i,R} \sigma^z_{j,R+1} \tag{28}$$

$$V_{\text{second n. Ring}} = \sum_R \sum_{i,j} \frac{1}{|\delta_{i,j,R,R+2}|^\alpha} \sigma^z_{i,R} \sigma^z_{j,R+2} \tag{29}$$

$$\tag{30}$$

To regain the full transverse-field long-range Ising Hamiltonian on the three ring system, we will now add the coupling between the spin-sites of the nearest neighbour rings and the next-nearest neighbour rings and a local transverse field perturbatively. On larger systems, the long-range aspect could be easily expanded by adding more coupling perturbations between rings with further distances. Therefore one gets the Hamiltonian H described by equations 25-30 of which the low-field ground-state behaviour will now be derived. By regarding the coupling between the rings one can see directly, that these processes do not change the state of the individual rings because they are diagonal in the basis of eigenstates of H_0. Therefore these perturbations do not generate or annihilate particles. They are only linking the individual rings. The field perturbation changes the state of one ring by flipping one of the n spin-sites. This could be interpreted in three different processes regarding the particle picture:

1. The field acts on a ground state where it flips one spin-site so that one gets an excited state (e. g. $\sigma^x_1 \langle\uparrow\downarrow\uparrow\downarrow| \rightarrow \langle\downarrow\downarrow\uparrow\downarrow|$). There is no possibility that a single application of the field on a ground state keeps the resulting state in the ground-state space. Therefore this is always a one-particle creation process.

2. The field acts on a excited state and flips one spin-site in a way that the resulting state is a ground state (e. g. $\sigma^x_2 \langle\uparrow\uparrow\uparrow\downarrow| \rightarrow \langle\uparrow\downarrow\uparrow\downarrow|$). This is a one-particle annihilation process.

3. The field acts on an excited state and the resulting state is still in the space of the excited states (e. g. $\sigma^x_3 \langle\downarrow\downarrow\uparrow\downarrow| \rightarrow \langle\downarrow\downarrow\downarrow\downarrow|$). This is a particle conserving process, which does not change the number of particles on the ring super-sites.

As the field-perturbation acts locally, one can understand these processes regarding matrix elements of the representation matrix of $\sum_i^n \sigma^x_i$ on one ring.

	ground states	excited states
ground states	T_0^{field}	T_{-1}^{field}
excited states	T_1^{field}	T_0^{field}

This is a good illustration to see the zero and one particle sector, but also to see how the particle creation and annihilation operators are locally realised in a representation matrix. One can now rewrite the Hamiltonian in equation 25 regarding particle operators on the rings.

$$H = H_0 + \frac{h}{J}\sum_R (T_{0,R}^{\text{field}} + T_{1,R}^{\text{field}} + T_{-1,R}^{\text{field}}) + \lambda_1 \sum_{R'} T_{0,R',R'+1}^{\text{nearest neighbour}} + \lambda_2 \sum_{R''} T_{0,R'',R''+2}^{\text{second n. neighbour}} \tag{31}$$

This is the Hamiltonian we will now treat with Takahashi's perturbation series-expansion method to investigate the effect of the perturbations on the degenerate ground-state manifold of H_0. The following considerations are done for the YC(4)-lattice because the solver tool that was used for the determination of the matrix elements requires an input of the amplitude for all the operations on all possible states. Hence one has to solve them exactly on one or two rings. Basically this evaluation could be done up to $n = 8$, but only for $n = 4$ the resulting number of matrix-elements is small enough to calculate the perturbation up to $\mathcal{O}(\lambda^{12})$ (or even $\mathcal{O}(\lambda^{13})$) in a acceptable amount of computation time. Order λ^n means the summation over all exponents of the perturbation parameters is equal n. In our considered system this means $h^i\lambda_1^j\lambda_2^k$ with $i+j+k=n$. We will see in the following sections that some important features of the system do not appear until such high orders.

As we are interested in the derivation of an effective low-energy model, it is useful to define a new pseudo-spin out of the ground states of the individual ring in the following way,

$$|\uparrow\downarrow\uparrow\downarrow\rangle \longrightarrow |\Uparrow\rangle \quad \text{and} \quad |\downarrow\uparrow\downarrow\uparrow\rangle \longrightarrow |\Downarrow\rangle \ . \tag{32}$$

It is now the approach to calculate the series expansion of all matrix-elements of combinations of $|\Uparrow\rangle$ and $|\Downarrow\rangle$ on the three ring system by using the matrix-element calculator named "Takahashi::TwoSideSolver"[4] and derive from these matrix-elements the effective 1D spin-chain model for the newly introduced pseudo-spins.

[4]The Solver is a tool developed and used by the AG Schmidt to compute solutions using the pCUT, Takahashi and Loewdin perturbation methods.

6.2 Matrix elements

The results of the calculation are series with powers of the three perturbation parameters h, λ_1 and λ_2 and coefficients depending on α. One must stress that for quantitative results it is necessary to calculate these coefficients for every regarded α. The perturbation order in which the matrix element appears is the summation over all three exponents of the perturbation parameters. There will be now a summary of matrix elements that are important and will generate terms in the effective low-energy model.
On the diagonal of the representation matrix of $\langle m_{R1}m_{R2}m_{R3}| H |m'_{R1}m'_{R2}m'_{R3}\rangle$ with $m_{Ri} \in \{\Uparrow, \Downarrow\}$ one finds in first-order the coupling with the second-nearest ring proportional to λ_2 like we have found in the zero field approach. It is important to stress that this is the only correction that is not proportional to h, therefore the only one that appears in the zero-field case. This fact was also already discussed in the zero field case.
At higher orders the main diagonal-contributions follow a specific rule: If the order is even, one finds constants that are not depending on the orientation of the pseudo-spins. If the order is odd the sign of the contribution depends on the orientation of m_{R1} and m_{R3}. At order nine and higher one also finds superpositions of these two cases. This means that the contribution changes its value, not only the sign, according to the orientation of m_{R1} and m_{R3}. At perturbation order 10 and 12 a new type of terms appears which depends on the orientation of m_{R1} relative to m_{R2} and m_{R_2} relative to m_{R_3}. This contribution is the first non-trivial coupling between nearest-neighbour rings.
The off-diagonal elements stand for processes where pseudo-spins are flipped. This means one ring changes its state from $|\uparrow\downarrow\uparrow\downarrow\rangle \rightarrow |\downarrow\uparrow\downarrow\uparrow\rangle$ or $|\downarrow\uparrow\downarrow\uparrow\rangle \rightarrow |\uparrow\downarrow\uparrow\downarrow\rangle$. The first non-diagonal matrix element one finds in every even order starting with order four. This process flips one pseudo-spin-site by flipping all real-spin sites of one ring due to the application of the transverse field h. At order nine two new processes appear on the off-diagonal. One of them flips a spin-site and the sign of the output results out of the orientation of both neighbours of that pseudo-spin-site. The other process flips the two sites m_{R1} and m_{R3} and provides a sign according to their orientation to each other. These processes appear in every odd order after order nine. In order ten we have found the last two contributions that will appear until order thirteen. One of these two contributions flips m_{R1} and m_{R3} without regarding their orientation to each other, and the other one changes the orientation of m_{R1} and m_{R2} in the same way. This was a brief introduction to all matrix elements, in the following chapter these results will be transformed to the pseudo-spin language of a 1D spin-chain.
One shall stress that we look at small perturbations, especially small field perturbations. Therefore one shall be aware of the fact that, the amplitude of processes appearing in higher order is smaller by magnitudes and the leading order matrix elements are the important one. Only if they vanish at certain α the higher order processes contribute to the ground state shape. For example at α_c such a situation will occur, and leading order terms will vanish. The exact impact of this will be investigated according to the effective model in the following section.

6.3 Effective 1D spin-chain

The ground states of individual rings were already introduced as pseudo-spins in equation 32. Now the formalism will be expanded by a set of pseudo-spin operations. These are similar to the application of Pauli matrices $\sigma^{x,y,z}\left|\uparrow\right\rangle$ to a regular spin, but to avoid misunderstandings in the notation of the effective language the Pauli operators are denoted by $\tau^{x,y,z}$ and are defined in the way described in figure 20.

τ^z	τ^x	τ^y
$\tau^z\left\|\Uparrow\right\rangle = 1\cdot\left\|\Uparrow\right\rangle$	$\tau^x\left\|\Uparrow\right\rangle = \left\|\Downarrow\right\rangle$	$\tau^y\left\|\Uparrow\right\rangle = i\cdot\left\|\Downarrow\right\rangle = i\cdot\tau^x\tau^z\left\|\Uparrow\right\rangle$
$\tau^z\left\|\Uparrow\right\rangle = -1\cdot\left\|\Uparrow\right\rangle$	$\tau^x\left\|\Downarrow\right\rangle = \left\|\Uparrow\right\rangle$	$\tau^y\left\|\Downarrow\right\rangle = -i\cdot\left\|\Uparrow\right\rangle = i\cdot\tau^x\tau^z\left\|\Downarrow\right\rangle$

Figure 20: Definition of τ operators on the pseudo-spins

Now the results of the matrix element evaluation are denoted in terms of τ operators. The coefficients are written in front of the effective operators in a general form. To make calculations with the effective model one has to evaluate these coefficients for every regarded α. The dependency on h, λ_1 and λ_2 of the coefficients is noted in brackets behind them. The number under each coefficient stands for the lowest order this term appears. In this thesis, we do not focus on the values of these coefficients because the system size is too small to gain correct results for quantitative values, but as discussed it is large enough to see the qualitative behaviour.
The diagonal elements can be translated into the effective language in the following way,

$$[\underbrace{E_0}_{0} + \underbrace{A_1(h)}_{2} + \underbrace{A_2(h,\lambda_2)}_{4} + \underbrace{A_3(h,\lambda_1)}_{6} + \underbrace{A_4(h,\lambda_1,\lambda_2)}_{8}]\mathbb{1} \tag{33}$$

$$[\underbrace{B_1(\lambda_2)}_{1} + \underbrace{B_2(h,\lambda_2)}_{3} + \underbrace{B_3(h,\lambda_1,\lambda_2)}_{7}]\sum_R \tau^z_R\tau^z_{R+2} \tag{34}$$

$$\underbrace{C_1(h,\lambda_1,\lambda_2)}_{10}\sum_R \tau^z_R\tau^z_{R+1} \quad . \tag{35}$$

The zeroth order and every diagonal entry that is not depending on the orientation of the pseudo-spins can be represented as an identity operator term. The matrix elements show that the coefficients A_{1-4} are always depending on h and the dependency on the coupling between the rings occurs at higher orders. This behaviour at least for the nearest-neighbour case could be interpreted in the following way. To couple the rings with each other, it is first necessary to excite the ground states of each ring, then link the excited stated states and then bring them back to the ground-state space.
The next-nearest neighbour $\tau^z\tau^z_{R+2}$ term already occurs in the zero-field case. Hence it has the only coefficient that is independent of h. This coupling is also possible with an application of the local field as B_2 shows. To also include a coupling with nearest-neighbour rings a higher order is necessary because nearest-neighbour coupling is just possible for excited states that have left the ground-state space due to field fluctuations. It is natural that this effective second-neighbour connecting term remains if the coupling between nearest rings is switched off ($\lambda_1 = 0$).
The nearest-neighbour Ising coupling $\tau^z\tau^z_{R+1}$ occurs not until order ten because it is necessary to excite and de-excite each of the three rings of the system, which makes

six perturbation processes including the field necessary. Then there are three nearest rings and one second-nearest ring coupling involved, what makes this process look like a coupling loop. One has to stress that this nearest neighbour coupling is way less relevant than the second-nearest neighbour Ising coupling $\tau^z\tau^z_{R+2}$. We can conclude from the effective diagonal terms (eq. 33-35), that we have found some terms that lead to an effective shift of E_0 in eq. 33 and a longitudinal coupling of the nearest ring and second-nearest ring eq. 34, 35. These processes are generalised straightforward to the coupling of rings with larger odd and even ring distance. Just the amplitude of these processes would get smaller due to the algebraic decay of the coupling.
Now the effective model for the off-diagonal processes is written down in equations 36-40.

$$[\underbrace{D_1(h)}_{4} + \underbrace{D_2(h,\lambda_2)}_{6} + \underbrace{D_3(h,\lambda_1)}_{8} + \underbrace{D_4(h,\lambda_1,\lambda_2)}_{10}] \sum_R \tau^x_R \tag{36}$$

$$\underbrace{\tilde{E}(h,\lambda_2)}_{9} \sum_R \tau^x_R\tau^z_R\tau^x_{R+2}\tau^z_{R+2} = \underbrace{E(h,\lambda_2)}_{9} \sum_R \tau^y_R\tau^y_{R+2} \tag{37}$$

$$\underbrace{F(h,\lambda_2)}_{10} \sum_R \tau^x_R\tau^x_{R+2} \tag{38}$$

$$[\underbrace{G_1(h,\lambda_1)}_{10} + \underbrace{G_2(h,\lambda_1,\lambda_2)}_{12}] \sum_R \tau^x_R\tau^x_{R+1} \tag{39}$$

$$\underbrace{H(h,\lambda_1,\lambda_2)}_{9} \sum_R \tau^z_{R-1}\tau^x_R\tau^z_{R+2} \tag{40}$$

As equation 36 shows, the first process that can flip one pseudo-spin appears in fourth order and results of four applications of the field in a ground state in the following way $\sigma^x_1\sigma^x_2\sigma^x_3\sigma^x_4 \left|\uparrow\downarrow\uparrow\downarrow\right\rangle = \left|\downarrow\uparrow\downarrow\uparrow\right\rangle$. Higher orders of this process could also contain more spin-flips and couplings between the rings as denoted in the dependencies of the coefficients D_{2-4} of $\lambda_{1,2}$. This process could be interpreted as an effective transverse field to the couplings described in 34 and 35.
Equations 37 and 38 show a next-nearest ring flip of two spin-sites. These processes require at least an eight-time application of the field. That implies that two spin-sites could only be flipped if there is a coupling between them. Equation 39 also underlines this for the nearest ring case. The difference between the $\tau^y\tau^y_{R+2}$ and the $\tau^x\tau^x_{R+2}$ term is that in case of τ^y the coupling between second-nearest ring is applied an odd number of times to generate the matrix element whereas in the τ^x case it is applied an even number of times.
In case of the $\tau^x\tau^x_{R+1}$ coupling for the nearest-ring case (eq. 39) the τ^y term does not appear in a lower order as the τ^x term. This difference to the second-nearest neighbour case results, because in the for second neighbour ring one always finds λ_2^k with $k \bmod 2 = 1$ terms before the $k \bmod 2 = 0$ terms. Therefore the $h^8\lambda_2$ appears in lower order than the $h^2\lambda_2^2$ term. Whereas for the nearest-ring coupling it is in general very rare to find odd potencies of λ_1 in the series of the matrix elements. However, one needs these terms to create a τ^y. Therefore the τ^x appears first. If a $\tau^y_R\tau^y_{R+1}$ would appear at all, it is at a much higher perturbation order than we can calculate.
One can interpret the $\tau^x_R\tau^x_{R+1,2}$ as couplings between the pseudo-spins in effective

field direction (eq. 39 and 38) described by equation 36. The $\tau_R^y \tau_{R+2}^y$ gives the second ring coupling even a third direction orthogonal to x and z.
The last part of the effective model is equation 40 and shows a cluster-state Hamiltonian on the 1D spin chain. Raussendorf and Briegel introduced this kind of Hamiltonian in the context of quantum computation in reference [19]. In quantum computation, this kind of operator is useful because it is highly entangled [20]. This ground state could be denoted as the state $|G\rangle$ that obeys the following rule [21],

$$S_i = \tau_{i-1}^z \tau_i^x \tau_{i+1}^z \qquad S_i |G\rangle = |G\rangle \quad \forall i \quad \text{and} \quad [S_i, S_j] = 0 \quad . \tag{41}$$

If a complete set of stabilizer operators S_i is provided the ground state is unique and called a cluster state. This is the case for periodic boundary conditions or infinite systems [21].

6.4 Discussion of the effective model

To interpret the effective model properly it is useful to summarise diagonal terms and off-diagonal terms to known 1D quantum spin models. The order in which the effective terms appear first is essential to their magnitudes. Equation 33 is as a H_0 ground-state energy correction not essentially important for the creation of new ground-state behaviour. If one looks at the coupling between the second-neighbour rings one finds a pure Ising pseudo-spin model up to order four (eq. 34) where one gets an additional effective transverse field (eq. 37),

$$H_{\text{eff}}^{\text{TF}} = J_{\text{eff}} \sum_R \tau_R^z \tau_{R+2}^z + h_{\text{eff}} \sum_R \tau_R^x \; . \tag{42}$$

This effective 1D chain realizes the stripe phases at the zero-field case depending on the sign of the coefficient J_{eff} in front of the $\sum_R \tau_R^z \tau_{R+2}^z$ term. If it is negative the zigzag-stripe phase is the ground state of the field-free model, if it is positive the second-nearest ring alternating plain-stripe order is the preferred one. It has to be stressed that these orders are the leading solutions on the considered space built up from the pseudo-spins. This part of the effective Hamiltonian splits the problem in two sub-lattices one of them are the rings with a odd ring number, the other sub-lattice are the one with an even ring-number. Due to the application of a field h, h_{eff} will also increase. At $h_{\text{eff}} = J_{\text{eff}}$ there is a 2D-Ising second-order phase transition to an effective x-polarized phase that will be now generalized to a long-range case. The full transverse-field chain, occurring at order four, for second nearest rings could be generalized to all cases of an even ring-distance that makes the results of Fey and Schmidt for a long-range transverse-field Ising chain applicable [22] although with a modified interaction decay function [17]. The authors show for the ferromagnetic case a phase transition between a z-polarized phase at low field and an x-polarized phase at high field. In the antiferromagnetic case the authors find an alternating Néel phase at low field and also an x-polarized phase at high field. In terms of stripe phases the z-polarized phase could be interpreted as zigzag stripes, because they obey the zigzag-stripe condition that the second-nearest pseudo-spin has the same orientation. On the other hand the Néel phase realizes the plain stripe order because every second-nearest ring has the opposite orientation. The x-polarized phase could be interpreted as a superposition of both possible ground states on each ring,

$$|\Rightarrow\rangle = \frac{1}{\sqrt{2}}(|\Uparrow\rangle + |\Downarrow\rangle) = \frac{1}{\sqrt{2}}(|\uparrow\downarrow\uparrow\downarrow\rangle + |\downarrow\uparrow\downarrow\uparrow\rangle) \; . \tag{43}$$

It is physically plausible that an effective x-polarized phase is adiabatically connected to the x-polarized phase on the YC(n)-lattice, because the effective transverse-field occurs due to the real transverse field. Therefore this superposition effect on the ground-state space should be a manifestation of the real x-polarized phase. This x-polarised phase with the second-order phase transition to the stripe phases occurs depending on the inclusion of couplings of further even ring distances, at different critical ratios of $\frac{h_{\text{eff}}}{J_{\text{eff}}}$. For the case of equation 42 the phase transition occurs at $h_{\text{eff}} = J_{\text{eff}}$. The corresponding h for which this phase transition occurs is now determined for $\alpha = 3$ by calculating $h_{\text{eff}}(h)$ and $J_{\text{eff}}(h)$ from the matrix element series expansion.

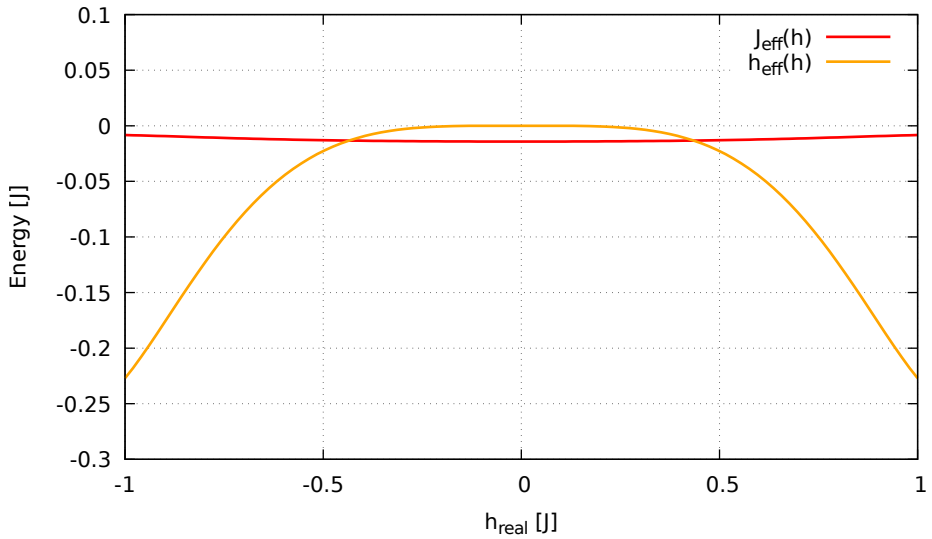

Figure 21: Plot of $h_{\text{eff}}(h)$ and $J_{\text{eff}}(h)$ for $\alpha = 3$; Change from the stripe phase to the effective x-polarized phase at $h_{\text{real}} \approx 0.43\,J$

In figure 21 one can see well the described phase transition at $h_{\text{real}} \approx 0.43\,J$ for the small cluster size. But also the connection between h and h_{eff}, because if h vanishes also h_{eff} vanishes. The evaluated value for the phase transition is just a reference value for the whole model including further couplings.

It is valid to consider the following high order terms as small, because they just appear in much higher perturbation order and we are regarding small h.
At order nine and ten the sums $\sum_R \tau^y_R \tau^y_{R+2}$ and $\sum_R \tau^x_R \tau^x_{R+2}$ extend the transverse-field Ising chain to a full XYZ-model,

$$H^{XYZ}_{\text{eff}} = \sum_R (J^x_{\text{eff}}\,\tau^x_R \tau^x_{R+2} + J^y_{\text{eff}}\,\tau^y_R \tau^y_{R+2} + J^z_{\text{eff}}\,\tau^z_R \tau^z_{R+2}) + h_{\text{eff}} \sum_R \tau^x_R \tag{44}$$

This model is subject of current research. Therefore the bleeding edge results of Shi, Li and Zhou [23] and Jafari [24] for the transverse-field free XYZ model are presented. In the limit of a high effective field, the same x-polarized order as in the transverse-field Ising chain will occur. The authors find for a Hamiltonian of the

following shape

$$H(J_x, J_y, J_z) = \sum_i (J_x \sigma_i^x \sigma_{i+1}^x + J_y \sigma_i^y \sigma_{i+1}^y + J_z \sigma_i^z \sigma_{i+1}^z) \quad , \tag{45}$$

that the ground state phase is determined by the largest $|J_\mu|$ with $\mu \in x, y, z$. The authors of [23] rewrite the Hamiltonian with new parameters

$$H(\gamma, \Delta) = \sum_i (\frac{1+\gamma}{2} \sigma_i^x \sigma_{i+1}^x + \frac{1-\gamma}{2} \sigma_i^y \sigma_{i+1}^y + \frac{\Delta}{2} \sigma_i^z \sigma_{i+1}^z) \quad , \tag{46}$$

to make it possible to visualise the phase transitions in a phase diagram by tuning $\gamma > 0$ and Δ as anisotropy parameters. Figure 22 shows the occurring phases depending on γ and Δ. With the $AF_{z,x}$-phase the authors mean a Néel-order phase in z,x-direction, whereas F_z stands for a z-polarized phase. What we now use is that the $\tau_R^z \tau_{R+2}^z$ coupling occurs in a much lower perturbation order, that is why the ferro- or antiferromagnetic z-order should be the dominating one like for the transverse-field Ising chain. If one looks at the values of the leading perturbative matrix elements, it seems that this is nearly everywhere true except for a small range around the critical α value.

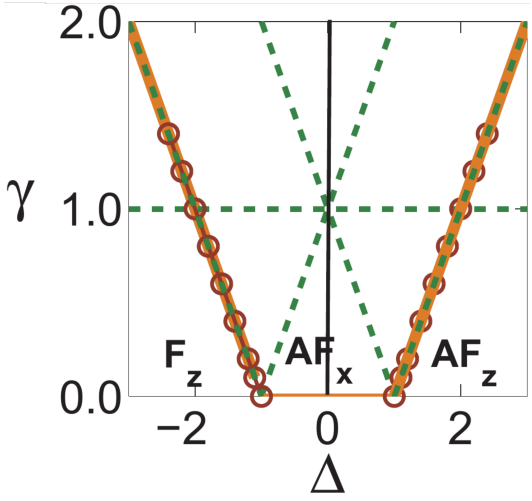

Figure 22: Ground-state phase diagram for the quantum-mechanical XYZ-model for spin-$\frac{1}{2}$. Solid lines denote the boundaries between distinct symmetry breaking phases (AF_x, AF_z, F_z)[23].

To determine the properties of the XYZ model close to the vicinity of to α_c, we look as an example, at the YC(4) effective model and the leading order matrix elements which are $\mathcal{O}(\lambda_2)$ for the z-coupling, $\mathcal{O}(h^8 \lambda_2^2)$ for the x and $\mathcal{O}(h^8 \lambda_2)$ for the y-coupling. The α values around the critical point are plotted in figure 23. One can directly see that at $\alpha = \alpha_c$ the matrix elements in z- and y-direction vanish. Only the coupling in effective field direction stays with the ferromagnetic sign. Therefore near the critical α the separated consideration of the second-nearest neighbour sub-lattice coupling leads to an effective x-polarized phase near the critical α also for small effective transverse-fields. The coupling between nearest neighbours underlines that polarisation because we find at tenth order a transverse-field XZ-model (equation 39, 36). That means a transverse-field Ising model with additional

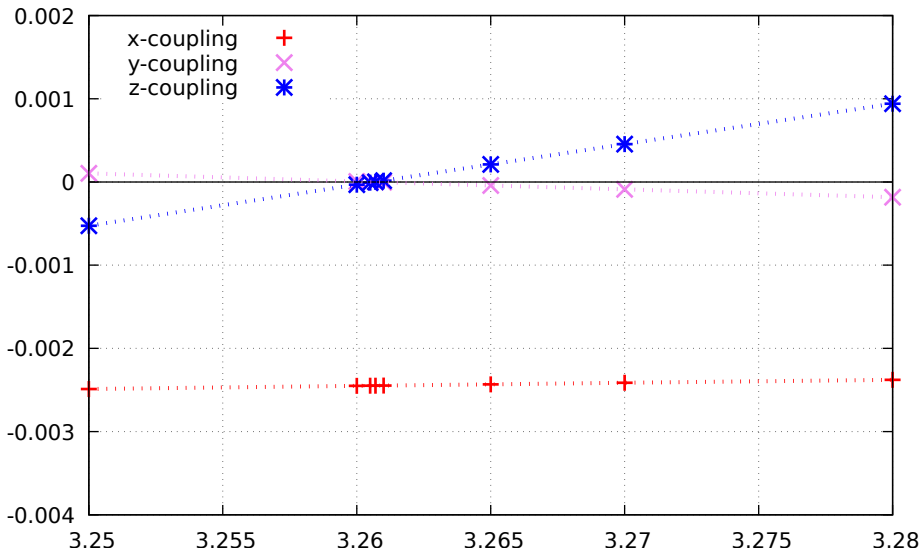

Figure 23: Plot of the leading order matrix elements near the critical α

coupling in field direction (35). The matrix elements of the coupling in field direction are also not vanishing at the critical α and is also of $\mathcal{O}(h^8)$. However, the coupling in the z-direction of $\mathcal{O}(h^6)$ is also not zero at α_c but two magnitudes smaller than the coupling in the x-direction. Therefore the x-polarized phase around α_c due to a field-fluctuation would be very likely, especially because the effective transverse-field is $\mathcal{O}(h^4)$.
The last term of the effective model is the cluster state Hamiltonian in equation 40, which has a unique highly entangled ground state of the following form

$$|\mathrm{GS}\rangle = \prod_i \frac{1 - (\tau^z_{i-1}\tau^x_i\tau^z_{i+1})}{2} |\mathrm{state}\rangle \quad . \tag{47}$$

Trough, it is important that the state on which the operators acts must not be orthogonal to the ground state. In case of open boundary conditions the ground state is four times degenerate . Son, Amico and Verdral investigated the cluster state operator on a 1D-chain under the aspect of symmetry and found that the degeneracy of the ground state is not affected by perturbations of the form $\{\tau^x_i, \tau^x_i\tau^x_j, \tau^z_i, \tau^z_i\tau^z_j, \tau^x_i\tau^z_j\}$ [25]. The ground state of this cluster-state Hamiltonian is adiabatically connected to the ground state of the transverse-field τ^x, hence it does not lead to new behaviour. This cluster-state Hamiltonian seems not important for the creation of a clock order phase because it has just a unique ground state with no phase transitions which is adiabatically connected to the x-polarized phase. But an assumed clock order would need a phase transitions from the stripe to the clock order and from the clock order to the field polarized order.
That means just the transverse-field Ising chain at nearest neighbour rings, or the XYZ-chain are left to create a possible clock order but it is not possible that only these two components do so, because if one looks, e. g. at a YC(6)-lattice in clock order and pick out one ring (analogous to figure 4). One can see in figure 24 that a translational invariant pattern with period three is necessary to get a clock order [8].

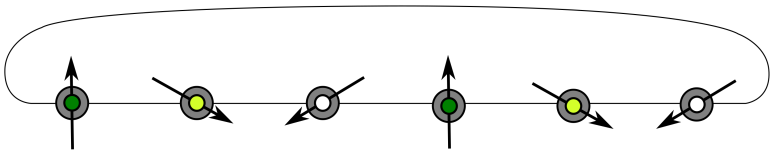

Figure 24: One ring as an excerpt of the YC(6)-lattice in clock-order state. Arrows symbolize the complex phase of the orientation of the one particle gap (results taken from [8] and [17]).

In any of the ground-state phases of the effective Ising chains the state of each ring is, considered separately, of the form,

$$|\mathrm{GS}\rangle = \frac{1}{\sqrt{a^*a + b^*b}}(a\,|\Uparrow\rangle + b\,|\Downarrow\rangle) = \frac{1}{\sqrt{a^*a + b^*b}}(a\,|\uparrow\downarrow\uparrow\downarrow\uparrow\downarrow\rangle + b\,|\downarrow\uparrow\downarrow\uparrow\downarrow\uparrow\rangle) \quad \text{with} \quad a, b \in \mathbb{C}\,. \tag{48}$$

It is clear that this superposition will not leave the ground-state manifold and the symmetry of the ground state of one ring will not break down to form the clock-order symmetry.
Thus we can conclude regarding the clock order, that the low-field Takahashi expansion in the chosen form is not capable of reproducing an indication for clock order. However, this shows that for the formation of clock ordering also the higher excitations of each ring are necessary. This also fits with the result of the zero-field Ising analysis of this thesis because at $\alpha = \infty$ the zero field Ising ground-state could consists also of "excited-rings" as long as the condition in eq. 10 is obeyed. The inclusion of these states in the zero field highly degenerate ground state favours the creation of clock ordering at the symmetry breaking by a field. If we now look at finite α, due to the long-range coupling the degeneracy of the ground state breaks down to the described stripe phases. This excludes the excited-rings of the ground state. Hence the formation of the clock order is energetically dependent on the formation of excited rings, what stabilises the ground state space created by the states where every ring is in the ground state against the order by disorder. That underlines the results of reference [2] and the occurring stripe-ordered phase at a small field that stabilises more with smaller α.
The last question that has to be answered is how the x-polarized order near the critical α could be interpreted regarding the results of reference [15] and [16]. The investigated effectively x-polarized phase appearing around α_C should be adiabatically connected to the real high field x-polarized phase. Hence we do not have the spacial relation that is needed for an extra nematic phase between the stripes and the x-polarized phase. So we can conclude that we see an x-polarized phase at high field for all α and with a small range around α_c where this phase also comes down to low h. At α_c the x-polarized phase is directly formed for any value of h. If one regards figure 19 with that knowledge one can say that in second order the vertical line at α_c is a singular line where the x-polarized phase is directly preferred for any transverse field.

7 Summary and Outlook

In this bachelor thesis, the long-range transverse-field Ising model on the YC(n)-lattice was investigated in the low-field limit, by reconstructing the whole Hamiltonian perturbatively from the zero-field ground states of one ring. The first part focused on the zero-field Ising Hamiltonian on the YC(n)-lattices which was exactly reconstructed by a first-order perturbation. The ground states of such a YC(n)-lattice at zero-field are depending on n and α four-fold degenerate zigzag stripes or plain stripes in the infinite direction. At zero field, if n is a multiple of four, one has a critical α_c were the stripe-shape changes with a first-order phase transition from the zigzag to the plain stripes with increasing α. If n is not a multiple of four or larger than 32 only plain stripes are the occurring order. Therefore, we propose the plain stripes, as a 6-fold degenerate ground state for 2D. The deduced ground-state space is also stable against a possible clock order for $\alpha < \infty$ because it needs a finite amount of energy to create excited states on the rings. The reason for this is that the space that is created by the ground states of individual rings does not contain the relevant states to create a clock order.
The other major point of interest was deriving an effective model by using the two ground states of a ring as an effective pseudo spin-$\frac{1}{2}$. That was done by Takahashi expansion for the nearest- and second-nearest ring coupling and results in an effective 1D transverse-field XYZ-model for the second-nearest ring coupling, a transverse-field XZ-model for the nearest-ring coupling and an additional 1D cluster state Hamiltonian. This effective model was not able to show an indication of the clock order but provides important information about the behaviour of the effective pseudo-spin space and its behaviour under the application of h and the phase transition at a finite field at α_c. We have found that away from α_c the respective stripe phases are stable due to field fluctuations in the ground state space, by finding the stable z-polarized or z-alternating order at the effective second-nearest ring coupling as a leading term of the perturbation. At α_c the z and y coupling vanish and at a finite field h only the x coupling remains. Therefore the x-polarized phase occurs at α_c for every finite h. In the vicinity around α_c the field that one needs to go to the x-polarized phase reduces, if one approaches α_c. We identified this phase as adiabatically connected to the real-spin model x-polarized phase, because the effective transverse field is in leading occurring order only depending on the real transverse field. Therefore at a finite field and α_c there no first order phase transition between the stripe phases, but a polarized phase between the stripe phases. The phase transition between the stripes and the x-polarized phase is a second-order phase transition within the 2D-Ising universality class. We find no evidence in our simple effective model of a nematic phase like in [16] for their artificial coupling parameter construction.
Therefore, we could verify the behaviour found by Saadatmand, Bartlett, and McCulloch of a stripe-phase occurring at finite h and specify precisely the ground state properties of a long-range interacting zero-field Ising Hamiltonian plus the low-field behaviour. We have also investigated that the occurring stripe phase is not a zigzag-stripe phase but a plain-stripe phase. However, it was not possible to create a model from this low-field limit that shows both a stripe-order and a clock order. The next step in the investigation of this model would be a perturbative expansion of the nearest-neighbour limit to finite α, because as we have seen that the exited rings

that are part of the pure Ising nearest-neighbour Ising model are the ones needed to create the clock order. The other task that is still pending is the systematic derivation of the effective model also for larger long-range interactions between the rings than the one with the second nearest ring. This would also lead to a further understanding of the processes underlying the x-polarized phase at α_c.
Another interesting aspect is the direct evaluation of the 2D-triangular lattice at low α to check how or if stripe phases can also occur in 2D at a finite field or to investigate the properties of a phase transition on a YC(n)-lattice between stripe phases and clock order and the universality class of such a phase transition.

8 Acknowledgements

I would like to thank my supervisors Sebastian Fey and Prof. Dr. Kai Phillip Schmidt as well as the whole AG-Schmidt for their great support and their open ear for all my questions. I would also like to thank all Theoretische Physik I members for the friendly inclusion of me in the everyday life of the department.

References

[1] J. W. Britton, B. C. Sawyer, A. C. Keith, J. Wang, J. K. Freericks, H. Uys, M. J. Biercuk, and J. J. Bollinger. Engineered two-dimensional Ising interactions in a trapped-ion quantum simulator with hundreds of spins. *Nature*, 484:489 EP –, Apr 2012.

[2] S. N. Saadatmand, S. D. Bartlett, and I. P. McCulloch. Phase diagram of the quantum Ising model with long-range interactions on an infinite-cylinder triangular lattice. *Physical Review B*, 97:155116, Apr 2018.

[3] S. Fey, S. Kapfer, and K. P. Schmidt. Quantum criticality of two-dimensional quantum magnets with long-range interactions. *arXiv preprint arXiv:1802.06684*, 2018.

[4] E. Ising. Beitrag zur Theorie des Ferromagnetismus. *Zeitschrift für Physik*, 31(1):253–258, Feb 1925.

[5] W. Lenz. Beitrag zum Verständnis der magnetischen Erscheinungen in festen Körpern. *Zeitschrift für Physik*, 21:613–615, 1920.

[6] S. G. Brush. History of the Lenz-Ising Model. *Reviews of Modern Physics*, 39:883–893, Oct 1967.

[7] P. Pfeuty. The one-dimensional Ising model with a transverse field. *Annals of Physics*, 57(1):79 – 90, 1970.

[8] M. Powalski, K. Coester, R. Moessner, and K. P. Schmidt. Disorder by disorder and flat bands in the kagome transverse field Ising model. *Physical Review B*, 87(5):054404, 2013.

[9] R. Moessner and S. L. Sondhi. Ising models of quantum frustration. *Physical Review B*, 63(22):224401, 2001.

[10] S. V. Isakov and R. Moessner. Interplay of quantum and thermal fluctuations in a frustrated magnet. *Physical Review B*, 68:104409, Sep 2003.

[11] Y. Shokef and T. C. Lubensky. Stripes, zigzags, and slow dynamics in buckled hard spheres. *Physical review letters*, 102(4):048303, 2009.

[12] M. Takahashi. Half-filled hubbard model at low temperature. *Journal of Physics C: Solid State Physics*, 10(8):1289, 1977.

[13] T. Kato. On the convergence of the perturbation method. I. *Progress of Theoretical Physics*, 4:514–523, 1949.

[14] T. Kato. *Perturbation theory for linear operators*, volume 132. Springer Science & Business Media, 2013.

[15] S. E. Korshunov. Nature of phase transitions in the striped phase of a triangular-lattice Ising antiferromagnet. *Physical Review B*, 72:144417, Oct 2005.

[16] A. Smerald, S. Korshunov, and F. Mila. Topological aspects of symmetry breaking in triangular-lattice Ising antiferromagnets. *Physical Review Letters*, 116:197201, May 2016.

[17] S. Fey. Private communication.

[18] I. P. McCulloch. Private communication between Kai P. Schmidt and Ian P. McCulloch.

[19] R. Raussendorf and H. J. Briegel. A One-Way Quantum Computer. *Physical Review Letters*, 86:5188–5191, May 2001.

[20] H. Kalis, D. Klagges, R. Orús, and K. P. Schmidt. Fate of the cluster state on the square lattice in a magnetic field. *Physical Review A*, 86(2):022317, 2012.

[21] D. Gottesman. Class of quantum error-correcting codes saturating the quantum Hamming bound. *Physical Review A*, 54:1862–1868, Sep 1996.

[22] S. Fey and K. P. Schmidt. Critical behavior of quantum magnets with long-range interactions in the thermodynamic limit. *Physical Review B*, 94(7):075156, 2016.

[23] Q. Shi, S. Li, and H. Zhou. Duality and ground-state phase diagram for the quantum XYZ model with arbitrary spin s in one spatial dimension. *arXiv preprint arXiv:1803.03935*, 2018.

[24] S. A. Jafari. Exact phase diagram and topological phase transitions of the XYZ spin chain. *arXiv preprint arXiv:1703.01420*, 2017.

[25] W. Son, L. Amico, and V. Vedral. Topological order in 1D Cluster state protected by symmetry. *Quantum Information Processing*, 11(6):1961–1968, 2012.

A State-generation code

```
def generate_state(state_number,spinsite_number):

    #initialize outputstate
    output_state=[]

    #generation binary number and transformation in a list
    state_number_string=str(format(state_number,'b'))
    while len(state_number_string)<spinsite_number:
        state_number_string="0"+state_number_string
    for i in range(0,(spinsite_number)):
        output_state.append(int(state_number_string[i]))

    #output
    return(output_state)
```

B Distance-decay function code

```
def distance-decay(spr,i1,i2,r_one,delta_r,cc_j,alpha):


    # check entry
    if delta_r<0:
        # wrong input error delta_r has to be positive
        print("error")
        return(0)
    if spr%2!=0 and spr<1:
        # wrong input error spr has to be even
        print("error")
        return(0)

    half=spr/2

    #same position on the ring
    if i1==i2:
        #ringdifference is even
        if delta_r%2==0:
            d=delta_r*math.sqrt(3)/2.
            return(1/(d)**alpha*cc_j)
        #ringdifference is odd
        if delta_r%2==1:
            d=math.sqrt(3./4.*(delta_r)**2+1./4.)
            return(1/(d)**alpha*cc_j)
        print("error")

    #opposite position on the ring
    if i1+half==i2 or i2+half==i1:
```

```
        #ringdifference is even
        if delta_r%2==1:
            d=math.sqrt(3./4.*(delta_r)**2+(half-0.5)**2)
            return(1/(d)**alpha*cc_j)
        #ringdifference is odd
        if delta_r%2==0:
            d=math.sqrt(3./4.*(delta_r)**2+(half)**2)
            return(1/(d)**alpha*cc_j)
        print("error")

    #first ring is even
    if r_one%2==0:
        for i in range(1,half):
            #ring two site plus i is ring one site
            if (i2+i)%spr==i1:
                #ringdifference is even
                if delta_r%2==0:
                    d=math.sqrt(3./4.*(delta_r)**2+i**2)
                    return(1/(d)**alpha*cc_j)
                #ringdifference is odd
                if delta_r%2==1:
                    d=math.sqrt(3./4.*(delta_r)**2+(i-0.5)**2)
                    return(1/(d)**alpha*cc_j)
                print("error")

            #ring one site plus i is ring two site
            if (i1+i)%spr==i2:
                if delta_r%2==0:
                    d=math.sqrt(3./4.*(delta_r)**2+i**2)
                    return(1/(d)**alpha*cc_j)
                if delta_r%2==1:
                    d=math.sqrt(3./4.*(delta_r)**2+(i+0.5)**2)
                    return(1/(d)**alpha*cc_j)
                print("error")

    #first ring is odd
    if r_one%2==1:
        for i in range(1,half):
            #ring two site plus i is ring one site
            if (i2+i)%spr==i1:
                #ringdifference is even
                if delta_r%2==0:
                    d=math.sqrt(3./4.*(delta_r)**2+i**2)
                    return(1/(d)**alpha*cc_j)
                #ringdifference is odd
                if delta_r%2==1:
                    d=math.sqrt(3./4.*(delta_r)**2+(i+0.5)**2)
                    return(1/(d)**alpha*cc_j)
```

```
            print("error")

        #ring one site plus i is ring two site
        if (i1+i)%spr==i2:
            #ringdifference is even
            if delta_r%2==0:
                d=math.sqrt(3./4.*(delta_r)**2+i**2)
                return(1/(d)**alpha*cc_j)
            if delta_r%2==1:
                d=math.sqrt(3./4.*(delta_r)**2+(i-0.5)**2)
                return(1/(d)**alpha*cc_j)
            print("error")
print("total-error")
return(0)
```